How Important is Vegetation Phenology for European Climate and Heat Waves?

Ruth Lorenz

ETH Zurich, Institute for Atmospheric and Climate Science, Zurich, Switzerland, and ARC Center of Excellence for Climate System Science, University of New South Wales, Sydney, Australia

Edouard L. Davin

ETH Zurich, Institute for Atmospheric and Climate Science, Zurich, Switzerland

David M. Lawrence

National Center for Atmospheric Research, Boulder, Colorado

Reto Stöckli

Federal Office of Meteorology and Climatology MeteoSwiss, Zurich, Switzerland

Sonia I. Seneviratne

ETH Zurich, Institute for Atmospheric and Climate Science, Zurich, Switzerland

(Manuscript received 7 January 2013, in final form 7 June 2013)

ABSTRACT

It has been hypothesized that vegetation phenology may play an important role for the midlatitude climate. This study investigates the impact of interannual and intraseasonal variations in phenology on European climate using regional climate model simulations. In addition, it assesses the relative importance of interannual variations in vegetation phenology and soil moisture on European summer climate.

It is found that drastic phenological changes have a smaller effect on mean summer and spring climate than extreme changes in soil moisture (roughly $1/4$ of the temperature anomaly induced by soil moisture changes). However, the impact of phenological anomalies during heat waves is found to be more important. Generally, late and weak greening has amplifying effects and early and strong greening has dampening effects on heat waves; however, regional variations are found. The experiments suggest that in the extreme hot 2003 (western and central Europe) and 2007 (southeastern Europe) summers the decrease in leaf area index amplified the heat wave peaks by about 0.5°C for daily maximum temperatures (about half of the effect induced by soil moisture deficit). In contrast to earlier hypotheses, no anomalous early greening in spring 2003 is seen in the phenological dataset employed here. Hence, the results indicate that vegetation feedbacks amplified the 2003 heat wave but were not responsible for its initiation. In conclusion, the results suggest that phenology has a limited effect on European mean summer climate, but its impact can be as important as that induced by soil moisture anomalies in the context of specific extreme events.

1. Introduction

The land surface and the atmosphere form a coupled system. Land surface processes can affect climate through exchanges of water, energy, and chemical compounds (e.g., Pielke et al. 1998; Arora 2002; Arneth et al. 2010; Seneviratne et al. 2010). In particular, soil moisture–vegetation interactions can be critical in affecting these exchanges. Plants extract water and nutrients from the soil and exchange CO_2 and water through their leaf stomates. The regulation of these exchanges is driven, among other factors, by solar radiation, temperature, soil moisture (SM), and air humidity (e.g., Sellers et al. 1997). In addition, the plants strongly affect the radiative and aerodynamic properties of the land surface,

Corresponding author address: Ruth Lorenz, ARC Center of Excellence for Climate System Science, Level 4 Mathews Bld., University of New South Wales, Sydney, NSW 2052, Australia.
E-mail: r.lorenz@unsw.edu.au

which is also relevant for land–climate feedbacks (e.g., Betts et al. 2007; Davin and de Noblet-Ducoudré 2010).

Vegetation–climate feedbacks have been investigated on regional and global scales by using climate models as well as observations. For instance, the conversion of natural ecosystems into agricultural land affects regional climate through impacts on surface albedo, radiative forcing, or the partitioning of available energy into the sensible (H) and latent heat (λE) fluxes (Pitman et al. 2009; de Noblet-Ducoudré et al. 2012). On shorter time scales, leaf phenology could play a significant role in vegetation–climate feedbacks (e.g., Bonan 2008, chapter 26.4). For instance, Levis and Bonan (2004) have shown that the timing of leaf emergence has an impact on springtime temperature. Depending on prevailing weather conditions, in mainly temperature and precipitation, the timing of leaf emergence and senescence as well as the amount of leaves [expressed as, e.g., leaf area index (LAI); i.e., the total leaf area per land area ($m^2\,m^{-2}$)] can vary from year to year (e.g., Stöckli and Vidale 2004).

It has been found that interannual LAI variations primarily modify the partitioning of net radiation into sensible and latent heat fluxes, which in turn can influence local climate conditions (Buermann et al. 2001). Using a land surface model, Guillevic et al. (2002) showed that the influence of interannual variability in LAI on evapotranspiration strongly depends on the region considered. They found that evapotranspiration is sensitive to variations in vegetation state in wet regions that are not densely vegetated. The model used showed a reduced sensitivity due to a saturation effect over dense vegetation covers, such as tropical forests. In arid and semiarid regions the models sensitivity was reduced due to physiological control linked to environmental stress. Weiss et al. (2012) showed that a realistic representation of vegetation phenology positively influences the simulation of evapotranspiration. Boussetta et al. (2012) found that the forecast of near-surface air temperature and humidity is improved when a realistic LAI from satellite data is used.

Zaitchik et al. (2006) proposed that an early green-up in spring 2003, due to anomalous warm temperatures, enhanced soil drying and contributed to an increase in sensible heat flux in the following months, which enhanced the European 2003 summer heat anomaly. The latter event consisted of two heat waves, one in June and another in August. The late summer drought in 2003 led to a net reduction in LAI, especially over crops and pastures, further decreasing evapotranspiration and increasing temperature over these areas. The work of Stefanon et al. (2012) was to our knowledge the first study to investigate the effects of dynamic phenology on temperature anomalies in France during the 2003 heat

waves. They found that phenology dampened the June heat wave but amplified the August heat wave.

In this study, we use a regional climate model (RCM) coupled to a third-generation land surface model (COSMO-CLM²; see model name explanation in section 2a) to investigate impacts of phenology on European climate. We thereby focus on biogeophysical processes on monthly to yearly time scales. The model does not calculate vegetation phenology interactively; instead, we use a new LAI dataset with daily data over 50 yr (Stöckli et al. 2011) to prescribe phenology in the model. This setup allows us to perform model experiments with realistic LAI interannual variability. In addition, we perform sensitivity experiments removing the interannual variability in LAI (prescribed mean, maximum, and minimum seasonal cycles). In contrast to other studies investigating vegetation–climate feedbacks, the analysis not only focuses on effects on mean summer climate, but also examines the effect of LAI variability on specific extreme events. Furthermore, we use experiments with prescribed soil moisture to compare the effects of vegetation phenology versus soil moisture dynamics.

The outline of the study is as follows: section 2 describes the model and employed dataset as well as the performed model experiments. In section 3, we investigate effects from vegetation phenology on mean summer climate. The effects of LAI changes on temperature extremes are discussed in section 4. We investigate effects from vegetation phenology on climate in connection with heat waves and compare them to impacts of soil moisture–climate feedbacks. Finally, we analyze in more detail the respective feedbacks during the 2003 and 2007 European summer heat waves and droughts. Section 5 presents the discussion of the main results and the conclusions.

2. Methods and data

a. Model description

We use the COSMO-CLM² RCM (Davin et al. 2011; Davin and Seneviratne 2012). COSMO-CLM² consists of the nonhydrostatic RCM COSMO-CLM [the Consortium for Small-scale Modeling (COSMO) model in climate mode; Rockel et al. 2008], version 4.8.11, coupled to the Community Land Model, version 3.5 (CLM3.5, Oleson et al. 2008). CLM3.5 is a third-generation land surface model (LSM) representing hydrological, biogeophysical, and biogeochemical processes that determine the exchange of radiation, heat, water, and chemical compounds between the land and the atmosphere. CLM3.5 resolves more processes than the standard land surface scheme in COSMO-CLM and its overall structure
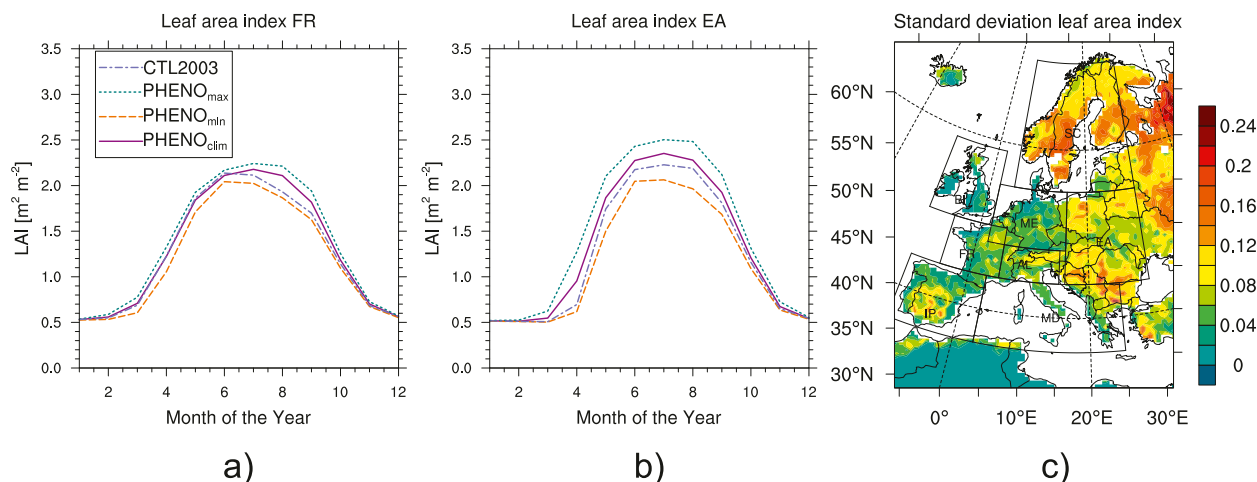
FIG. 1. Seasonal cycles in LAI over (a) France and (b) eastern Europe for the climatology of the LAI dataset (PHENO$_{clim}$), the minimum (PHENO$_{min}$) and maximum (PHENO$_{max}$) range, and the year 2003. (c) The interannual variability in LAI and the areas of the PRUDENCE domains.

is more complex. Most importantly, CLM3.5 contains an explicit link between stomatal conductance and photosynthesis. The version of COSMO-CLM^2 used in this study has been evaluated over Europe by Davin and Seneviratne (2012) and Lorenz et al. (2012). The use of CLM3.5 improves the simulation of several variables (e.g., surface fluxes, radiation fluxes, temperature, and precipitation). The main improvement in COSMO-CLM^2 over the standard COSMO-CLM is a better partitioning of the turbulent fluxes.

COSMO-CLM^2 offers several options related to the dynamical core and physical packages. We use the second-order leapfrog scheme for time integration. Vertical turbulent mixing is parameterized by a level-2.5 closure using turbulent kinetic energy as prognostic variable (Mellor and Yamada 1974, 1982). The mass flux scheme of Tiedtke (1989) is used for moist convection and large-scale precipitation is parameterized with a four-category one-moment cloud–ice scheme including clouds and rainwater, snow, and ice. CLM3.5 is used here without carbon–nitrogen dynamics and ecosystem dynamics; hence, LAI is not calculated interactively and is prescribed based on satellite data instead.

b. Leaf area index dataset

The default LAI dataset in CLM3.5 is based on Moderate Resolution Imaging Spectroradiometer (MODIS) satellite data and contains only a monthly climatology (Lawrence and Chase 2007). In this study, the default dataset is replaced with a new global reanalysis of vegetation phenology presented in Stöckli et al. (2011). This newer product covers 50 yr by using a prognostic phenology model driven by European Centre for Medium-Range

Weather Forecasts (ECMWF) Interim Re-Analysis (ERA-Interim) and 40-yr ECMWF Re-Analysis (ERA-40) meteorological data. The phenology model is constrained by 10 years of quality screened MODIS observations and delivers a daily LAI dataset with a mean LAI uncertainty of $0.34\,m^2\,m^{-2}$. The same subgrid-scale representation of plant functional types (PFTs) as in CLM3.5 is used and the dataset contains values per individual PFT. The final dataset contains 50 yr of daily $1° \times 1°$ global phenology with photosynthetically active radiation (FPAR) and LAI, as well as their uncertainty. For details on the method see Stöckli et al. (2011).

Figure 1 shows the annual cycle of LAI statistics for two subdomains in Europe [Figs. 1a,b; subdomains France and eastern Europe from the Prediction of Regional Scenarios and Uncertainties for Defining European Climate Change Risks and Effects (PRUDENCE) project; see section 2e(2) for definition and Fig. 1c for areas on map]. We display the climatology, minimum and maximum range, and as an example the year 2003 (which displayed a major drought and two heat waves; see also section 1). The drop in LAI was most pronounced in France during 2003 (Fig. 1a). The range between all-time minimum and maximum LAI is largest in eastern Europe. This can also be seen in Fig. 1c, which shows the standard deviation in LAI over the whole domain during summer, hence, the interannual summer LAI variability. The variability is largest in eastern Europe, the Balkans, and Scandinavia. However, generally the variability in our dataset is rather small compared to other, satellite-only-based, datasets (e.g., Buermann et al. 2001; Guillevic et al. 2002).

TABLE 1. Overview of experiments.

Short name	Interactive SM	Interannual varying LAI	Description
CTL	✔	✔	Reference run with daily LAI values with interannual variability (Stöckli et al. 2011) and interactive SM
PHENO$_{clim}$	✔		Daily seasonal cycle of LAI from CTL
PHENO$_{min}$	✔		Lowest LAI values of day of the year out of the total time series from CTL for each day of the year, minimum experiment
PHENO$_{max}$	✔		Highest LAI values of day of the year out of the total time series from CTL for each day of the year, maximum experiment
PHENO$_{zero}$	✔		LAI always zero, extreme experiment to test model sensitivity
PHENO$_{old}$	✔		LAI based on older, default dataset (Lawrence and Chase 2007)
SM$_{clim}$		✔	Soil moisture prescribed to seasonal cycle from CTL, LAI as in CTL
DRY		✔	Extreme dry run where SM is prescribed to 0.05% by volume, LAI as in CTL

c. E-OBS observations

We use the E-OBS gridded version 8.0 of the European Climate Assessment and Dataset (ECA&D; Haylock et al. 2008) to validate the 2003 and 2007 maximum daily temperature anomalies. E-OBS is a daily gridded observational dataset for precipitation and temperature in Europe based on ECA&D information. The full dataset covers the period 1950–2012.

d. Experimental setup

We performed several model runs with COSMO-CLM^2 (Table 1). The reference run (CTL) uses the LAI dataset of Stöckli et al. (2011) including interannual variability and calculates SM interactively. Experiment PHENO$_{clim}$ is the same as CTL except that the interannual variability of LAI has been removed by using the daily climatology (1989–2010) from CTL. Similarly, in experiments PHENO$_{min}$ and PHENO$_{max}$ a daily climatology of LAI is also prescribed. PHENO$_{max}$ (PHENO$_{min}$) uses for each day of the year the highest (lowest) LAI values out of the 1989–2010 time series, hence, a maximum (minimum) seasonal cycle. Thus, PHENO$_{min}$ represents late and weak greening of the vegetation and early senescence, while PHENO$_{max}$ represents early and strong greening of the vegetation and late senescence. PHENO$_{zero}$ is an extreme experiment to test the model sensitivity when LAI is always set to zero. Finally, PHENO$_{old}$ uses the default LAI dataset from Lawrence and Chase (2007) used in the Community Land Model in order to assess the sensitivity of the modeled climate to the prescribed LAI dataset.

Note that our setup does not allow for phenological feedbacks strictu sensu, since LAI is prescribed in the simulations and not dynamically computed by the model. However, the impact of phenology anomalies in single years (e.g., during the extreme 2003 and 2007 events, to be discussed hereafter) can be considered as feedbacks, because they result from the (observed) response of phenology to the respective climate anomalies during these events. This prerequisite holds as long as the climate anomalies remain similar in the different model runs, which is complied with in the present case.

In addition, experiments with prescribed SM and, therefore, no influence from the atmosphere on the SM state were also performed (using a common approach to decouple land and atmosphere; e.g., Koster et al. 2004; Seneviratne et al. 2006; Jaeger and Seneviratne 2011; Lorenz et al. 2012). These experiments use the same set up as CTL, except that SM is prescribed at very low (DRY) or climatological values (SM$_{clim}$). In the DRY run, SM is prescribed to very low values of 0.05% by volume, to represent an extreme dry situation. SM$_{clim}$ is more realistic and uses the SM climatological cycle from CTL (1990–2010). In SM$_{clim}$, both soil liquid and soil ice content are prescribed to the climatological values from CTL. The difference between PHENO$_{clim}$ and CTL corresponds to the effect of interannual variability in LAI, while the difference between SM$_{clim}$ and CTL corresponds to the effect of interannual variability in SM. But whereas LAI is prescribed in SM$_{clim}$, SM is interactive in PHENO$_{clim}$.

All model runs have 0.44° (~50 km) horizontal resolution, 32 vertical atmospheric layers, and a model time step of 240 s. Lateral boundary conditions were derived from ERA-Interim reanalysis data (Dee et al. 2011). This is the latest ECMWF global atmospheric reanalysis, covering the data-rich period since 1979, and continuing in real time. All simulations cover the years 1989–2010. The first year is used as spinup and only data from 1990–2010 are analyzed.

e. Analysis methodology

1) TEMPORAL AVERAGING

Generally, we analyze the simulations over seasons, using June–August (JJA) for summer and March–May (MAM) for spring. The mean of the corresponding

TABLE 2. Overview of heat wave indices shown in the figures.

Name	Definition
hwdi	Mean heat wave duration where daily maximum temperature is above the long-term 90th percentile from the reference run.
hwdi⋆	Mean heat wave duration index where daily maximum temperature is above the long-term 90th percentile from the respective run itself.
hot spells	Mean heat wave duration where daily maximum and daily minimum temperature are above the long-term 90th percentile from the reference run.
hot spells⋆	Mean heat wave duration where daily maximum and daily minimum temperature are above the long-term 90th percentile from the respective run itself.

variables is calculated over the respective months over the period 1990–2010. As a measure for interannual climate variability we use the interannual standard deviation (σ) of the respective variables.

2) SPATIAL AVERAGING

To analyze data over particular regions we use the PRUDENCE domains for spatial averaging. These European subdomains are defined in Christensen and Christensen (2007) and elsewhere and include eight regions: Britain and Ireland (BI), Iberian Peninsula (IP), France (FR), mid-Europe (ME), Scandinavia (SC), Alps (AL), Mediterranean (MD), and eastern Europe (EA). The exact regions are indicated in the map in Fig. 1c.

3) HEAT WAVE DURATION INDICES

We use several heat wave duration indices (Table 2). The exact definition of a heat wave index can have a crucial influence on the results of respective analyses (e.g., Lorenz et al. 2010; Perkins et al. 2012). Therefore, we check if our results are robust for several indices. We use indices in which the 90th percentile of daily temperatures is used as threshold to define if a day is considered as a hot day or not. For the heat wave duration

index (hwdi) and hot spells the 90th percentile is calculated from the reference run. For hwdi⋆ and hot spells⋆, the 90th percentile is calculated from the respective experiment, in order to remove the effect from the change in mean summer climate, that is, focusing on intrinsic persistence of the hot day anomalies for the respective runs (see also Lorenz et al. 2010). Then, we investigate the mean duration of heat waves over the time series at each grid point. For hwdi we only look at daily maximum temperature, for the hot spells also minimum daily temperatures are considered (to investigate heat waves with hot days and warm nights). Only heat waves where the 90th percentile threshold is exceeded for at least two consecutive days (and nights for hot spells) are taken into account.

3. Effect of LAI and SM changes on mean summer climate

a. Model sensitivity to vegetation phenology changes

The experiment with zero LAI (PHENO$_{zero}$) shows that the simulated mean summer climate is not very sensitive even to extreme vegetation changes (Fig. 2).
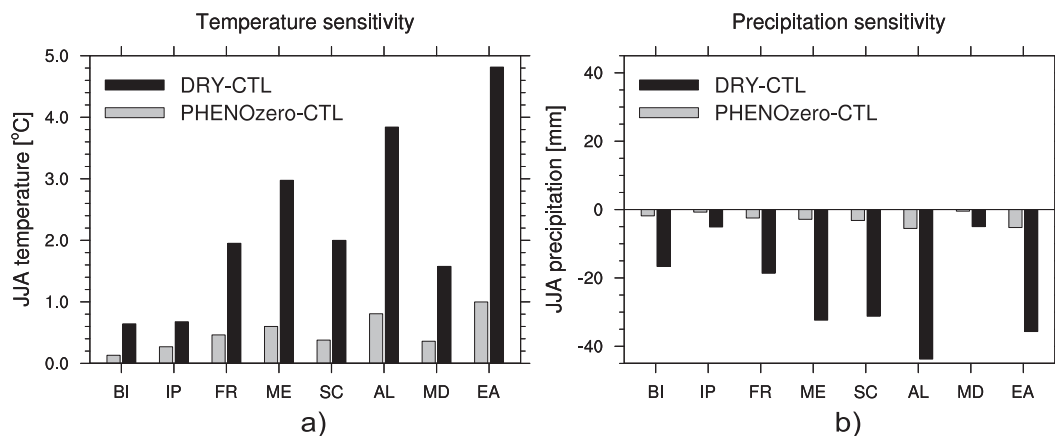

FIG. 2. Mean JJA regional averages (a) 2-m temperature and (b) precipitation for PHENO$_{zero}$ vs CTL (gray) and DRY vs CTL (black).

Temperature is increased as expected but at most by 1°C (Fig. 2a). Precipitation is decreased over most of Europe, but the differences to the reference run are small (Fig. 2b). Figure 2 also includes the corresponding results for experiment DRY. In the DRY run temperature changes reach up to 5°C (Fig. 2a) and precipitation is decreased by up to 40 mm per month (Fig. 2b). Hence, the model's mean summer climate is substantially more sensitive to extreme SM changes than LAI (by a factor of about 3–5 for temperature and 6–8 for precipitation, depending on the geographical region). In addition, we note that replacing the default Lawrence and Chase (2007) LAI dataset by the dataset of Stöckli et al. (2011) has a rather small impact on the simulated climate (i.e., for CTL versus $PHENO_{old}$; see appendix A, especially Fig. A2) and that model performance compared to observations is not substantially affected (Fig. A3). Hence, using realistic, yearly varying LAI data does not lead to a clear improvement or a decline in model performance in our experiments, at least for mean summer climate. However, the performed sensitivity experiments suggest that the prescribing of realistic daily phenology fields can be relevant for capturing extreme events (see below).

One reason for the smaller impact of LAI versus SM is the compensating mechanism provided by ground evaporation. In experiment DRY, both ground evaporation and transpiration get close to zero, whereas in $PHENO_{zero}$ transpiration and interception are switched off but ground evaporation is increased, thus maintaining evaporation at a substantial level. The fact that ground evaporation compensates for the decrease in transpiration to such a large degree in the model may be questioned and has been identified as a possible deficiency in CLM (Lawrence and Chase 2009; Boisier et al. 2012). Indeed, as CLM3.5 is currently parameterized, capillary forces can efficiently bring moisture from deep water stores up to the surface, maintaining relatively high ground evaporation even during periods of no rain (Oleson et al. 2008; Lawrence et al. 2011). Hence, although experiment $PHENO_{zero}$ is meant to capture the maximum effect potentially arising from changes in LAI, the effect may still be larger in reality than in the model.

b. Minimum (PHENO_min) and maximum (PHENO_max) LAI experiments

Compared to CTL, $PHENO_{min}$ and $PHENO_{max}$ represent cases with maximum or minimum LAI, respectively. In $PHENO_{min}$, smaller LAI compared to CTL leads to a decrease in transpiration (Fig. 3a). The resulting enhancement in ground evaporation compensates a large fraction of this decrease in transpiration (Fig. 3c), resulting in only about a 1–3 W m^{-2} drop in

latent heat flux (λE; Fig. 3e). The decrease in λE and the resulting increase in 2-m temperature (T_{2m}; Fig. 4a) are most pronounced around the Black Sea. The 2-m temperature shows a slight increase in $PHENO_{min}$. The daily minimum temperature (T_{min}) is also increased whereas this effect is larger than the impact on T_{2m} (Fig. 4c).

Figures 1a and 1b show that the rise in LAI in $PHENO_{max}$ compared to CTL is smaller than the decrease in $PHENO_{min}$ (because minimum LAI is farther away from the LAI climatology than the maximum LAI). Accordingly, the increase in transpiration (Fig. 3b) and the decrease in ground evaporation (Fig. 3d) in $PHENO_{max}$ are smaller than the opposite effects in $PHENO_{min}$. Additionally, $PHENO_{max}$ also shows regions with increased ground evaporation, even though the main signal is a decrease. These regions result in a clear increase in latent heat flux in $PHENO_{max}$ (Fig. 3f). However, the resulting net change in latent heat flux is very similar in magnitude in both experiments. The decrease in T_{2m} in $PHENO_{max}$ (Fig. 4b) is limited to southern and eastern Europe. As in $PHENO_{min}$, T_{min} is slightly more affected than T_{2m} (Fig. 4d).

In addition to temperature, Figs. 4e and 4f show the soil moisture index (SMI). SMI expresses soil moisture relative to field capacity (FC) and plant wilting point (PWP) as SMI = $(\Theta - \Theta_{PWP})/(\Theta_{FC} - \Theta_{PWP})$, where Θ is soil moisture in volumetric water content. SMI describes soil moisture within the available water capacity and therefore the water stress for vegetation (SMI = 1: no stress; SMI = 0: no water available; e.g., Betts 2004; Seneviratne et al. 2010). SMI was calculated over the first eight soil levels, which correspond approximately to the root depth. The differences in SMI for the phenology experiments are small. However, the pattern shows where more or less moisture stays in the soil due to the change in LAI. In $PHENO_{min}$ increased SMI compared to CTL dominates, reflecting the decrease in evapotranspiration (which leads to more SM remaining in the soil). The regions in $PHENO_{max}$ where SMI is decreased are about as large as regions with increased SMI. Regions where the largest increase in latent heat flux occurs in $PHENO_{max}$ (Fig. 3f) correspond to regions where SMI is increased (Fig. 4f). These are the regions where the increase in LAI does not lead to enhanced SM depletion but to increased SM at the end. In general, total evapotranspiration decreases when LAI is lower and increases when LAI is higher. However, the density and activity of vegetation cover have not only a direct effect on transpiration, but also an indirect effect on ground evaporation via impacts on SM and shading of the ground (Notaro et al. 2008; Liu et al. 2010). The net effect of vegetation state on total evapotranspiration, and thus also sensible heat flux, depends on additional
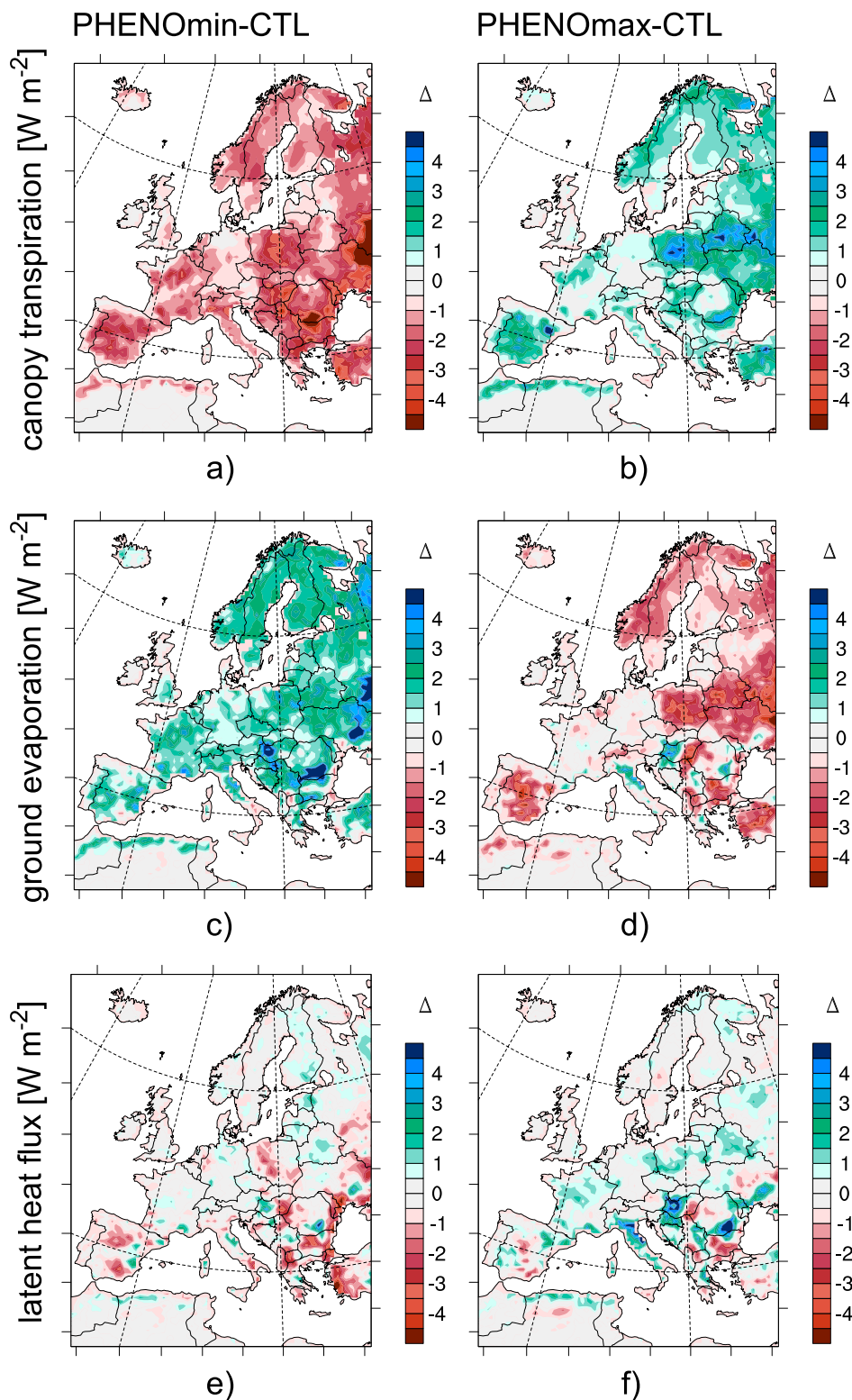
FIG. 3. Differences between (left) PHENO$_{min}$ and (right) PHENO$_{max}$ and CTL in mean summer (a),(b) canopy transpiration, (c),(d) ground evaporation, and (e),(f) latent heat flux.

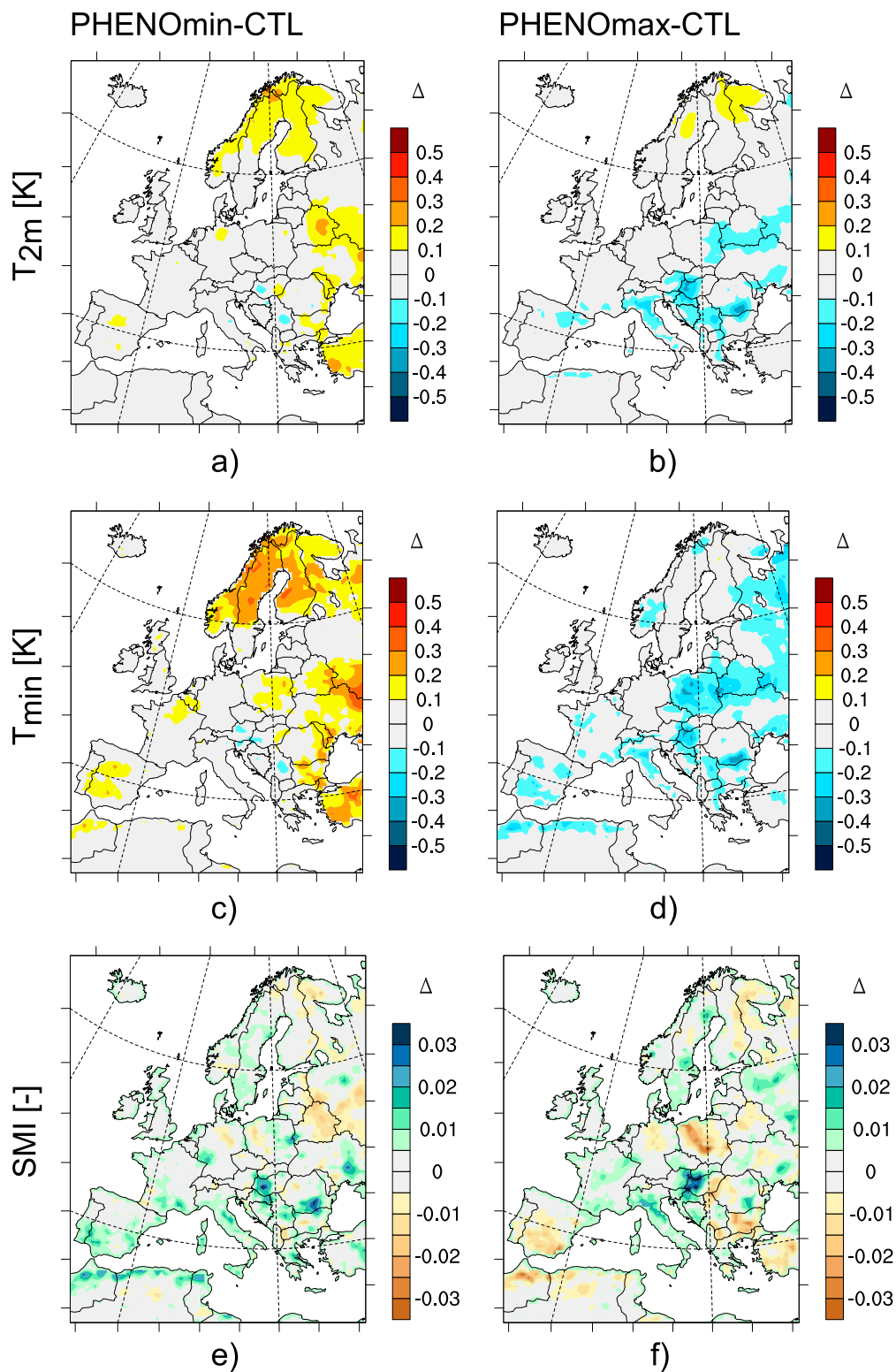PHENOmin-CTL   PHENOmax-CTL

FIG. 4. As in Fig. 3, but for (a),(b) 2-m temperature, (c),(d) daily minimum temperature, and (e),(f) soil moisture index.

factors such as climate conditions and land cover type and therefore varies among regions (Katul et al. 2012; Wang and Dickinson 2012). Consequently, there are large regional differences in the effects from a change in LAI.

The differences between the phenology experiments in spring are generally less pronounced than in summer and very small (and therefore not shown). The same effect as in summer occurs; that is, much of the change in transpiration is compensated by ground evaporation. This response could be specific to the model used because of the overcompensation of changes in transpiration by ground evaporation (as mentioned in section 3a), and effects during spring are possibly larger in reality.

The largest effect of increased or decreased LAI on mean summer climate is found for $T_{\min}$ in the PHENO$_{\min}$ experiment in Scandinavia and parts of eastern Europe (Fig. 4c). Note that $T_{\min}$ increases more than $T_{\max}$ and hence the diurnal temperature range (DTR) is decreased. The DTR has been shown to be sensitive to several factors, including land surface vegetation and moisture availability (Zhou et al. 2007, 2008; Zhang et al. 2009; Jaeger and Seneviratne 2011; Jeong et al. 2011). Zhou et al. (2007) propose that a decrease in either soil emissivity and/or vegetation cover would act to increase $T_{\min}$ more than $T_{\max}$. Soil moisture influences the thermal capacity of the soil. In dry conditions, daytime heat storage is increased as a result of less shading of the soil and more soil heating during the day. In wet conditions, longwave heat loss is decreased as a result of lower soil emissivity. In addition, a reduction in vegetation cover exposes more soil directly to the atmosphere, which increases the importance of the soil's emissivity for absorption and emission of longwave radiation. So, more heat is transferred from the soil to the atmosphere via H, increasing nighttime temperatures in particular. This mechanism can be applied to PHENO$_{\min}$ as well. Daily minimum temperatures usually occur shortly before sunrise and hence they are mostly affected by outgoing longwave radiation (LW$_{\text{out}}$). Note that LW$_{\text{out}}$ is higher in the less dense canopy of PHENO$_{\min}$ than in CTL in summer. Hence, in PHENO$_{\min}$ more energy is stored in the soil during the day that can be emitted during the night. Because of decreased (increased) LAI, LW$_{\text{out}}$ is increased (decreased) and therefore $T_{\min}$ is also increased (decreased).

c. Effect of removing interannual variability in phenology

The effect of removing the interannual variability in LAI on mean summer climate is shown in Figs. 5a,c,e and 6a,c,e. Since only the interannual variability in LAI is removed, while the mean LAI is conserved, no large

effects on the mean climate are expected. Indeed, the effect on mean summer climate is small. In southeastern Europe we obtain the clearest signal: ground evaporation is mainly decreased in this region, resulting in decreased λE (Figs. 5a,c,e). The corresponding increase in temperature is very small (Figs. 6a,c) and other regions display the opposite effect. In contrast to PHENO$_{\min}$ and PHENO$_{\max}$, removing interannual variability has a more pronounced effect on T_{2m} than $T_{\min}$. Only small differences in SMI are seen, the most pronounced one being a decrease in southeastern Europe that corresponds to the region where ground evaporation and latent heat flux are decreased in PHENO$_{\text{clim}}$. The effect on mean spring climate is even smaller than for summer (not shown).

d. Effect of removing interannual variability in SM

The effect of removing the interannual variability in SM on mean summer climate is shown in Figs. 5b,d,f and 6b,d,f. Canopy transpiration, ground evaporation, and latent heat flux all show the same pattern, an increase in southern Europe and a decrease in central and northern Europe (Figs. 5b,d,f). The effect on λE is more pronounced than for the phenology experiments since the changes in canopy transpiration and ground evaporation are of the same sign everywhere. The effect on temperature is also more pronounced, showing a clear, homogeneous, decrease in T_{2m} and $T_{\min}$ (Figs. 6b,d). There is almost no change in SMI between SM$_{\text{clim}}$ and CTL (Fig. 6f).

In the SM$_{\text{clim}}$ experiment evapotranspiration is generally not SM-limited, whereas we expect it to be in CTL in some summers. This thus causes the consistent increase in evapotranspiration seen in SM$_{\text{clim}}$ compared to CTL in southern Europe. The decrease in evapotranspiration in northern Europe is more difficult to explain and is caused by a limitation of the approach we use to prescribe SM. Soil ice and liquid water are prescribed individually; however, after these values are set the model adjusts the fraction of liquid and ice according to the temperature within one time step. In northern Europe evapotranspiration is energy limited and not SM limited. Temperature is overall decreased in SM$_{\text{clim}}$ (Figs. 6b,d). The overall decrease in temperature shows that the effect of making the dry years wetter is larger, in accordance with the fact that Europe generally is characterized by humid conditions and is only significantly modified under drier conditions. It also suggests that there are some nonlinearities in the European climate response to soil moisture (Jaeger and Seneviratne 2011). Because of this decrease in temperature, the proportion of the prescribed soil ice and soil liquid water does not correspond to the modeled temperature anymore and
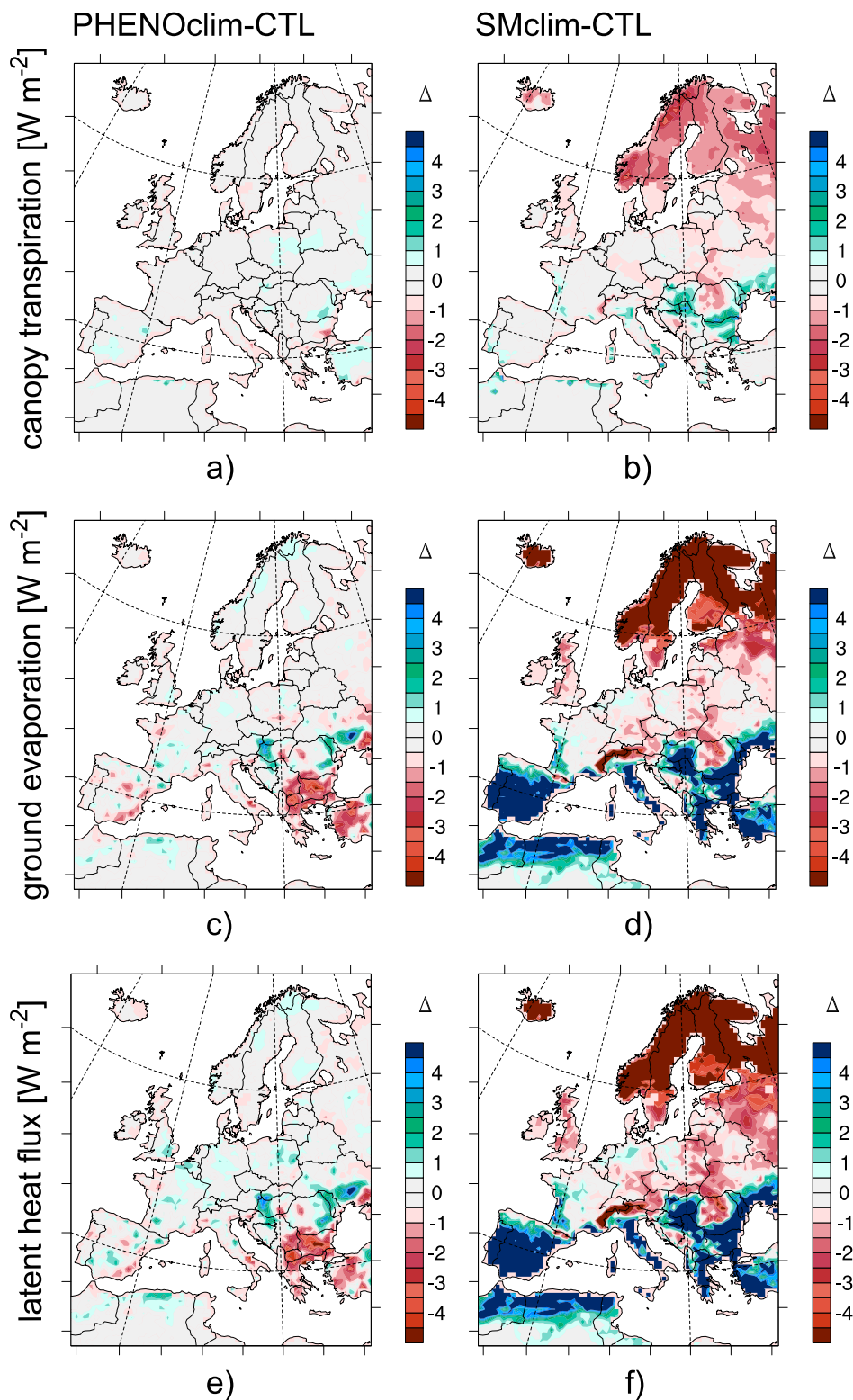
FIG. 5. Differences between (left) PHENO$_{clim}$ and CTL and (right) SM$_{clim}$ and CTL in mean summer (a),(b) canopy transpiration, (c),(d) ground evaporation, and (e),(f) latent heat flux.
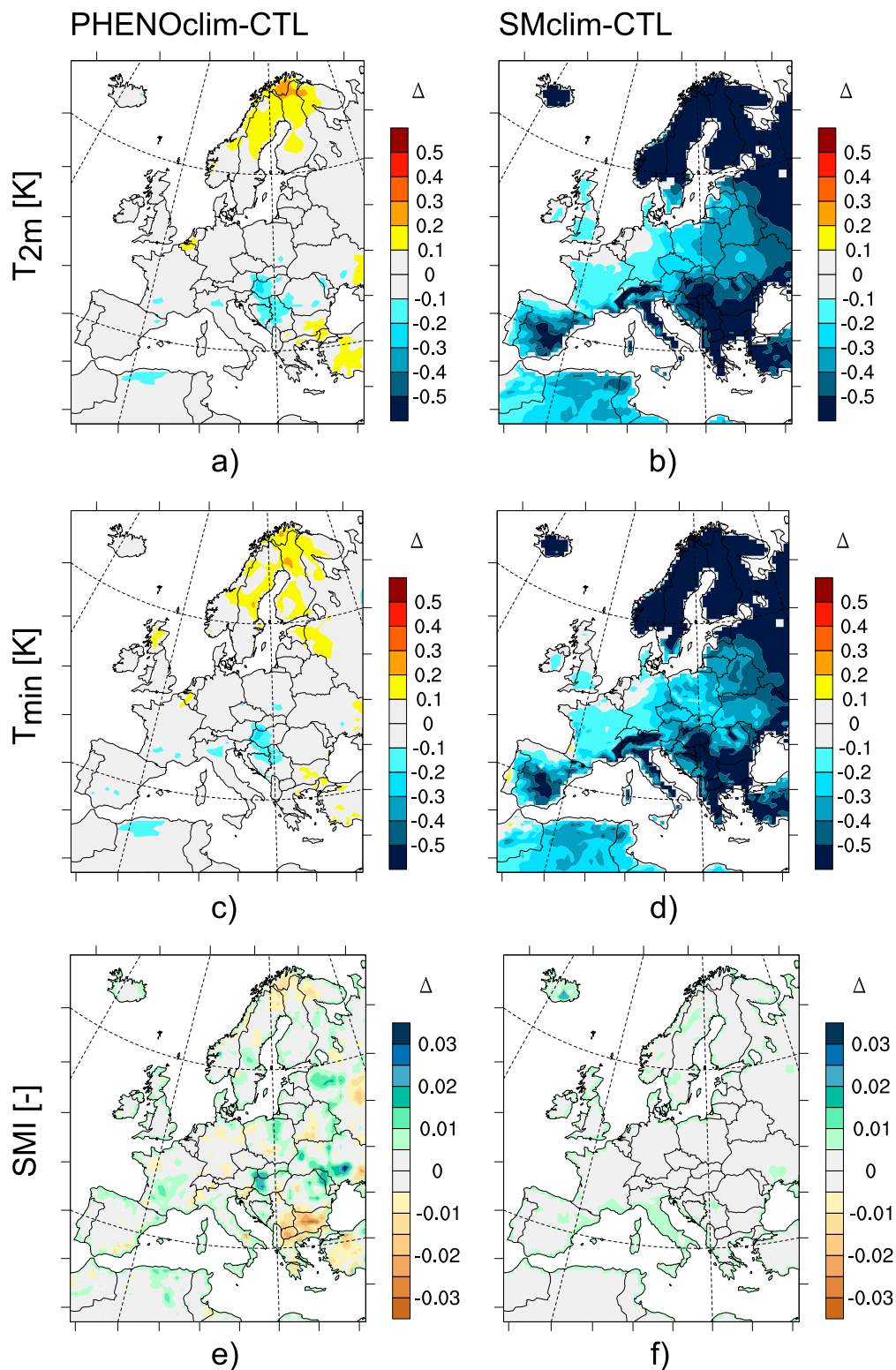
FIG. 6. As in Fig. 5, but for (a),(b) 2-m temperature, (c),(d) daily minimum temperature, and (e),(f) soil moisture index.
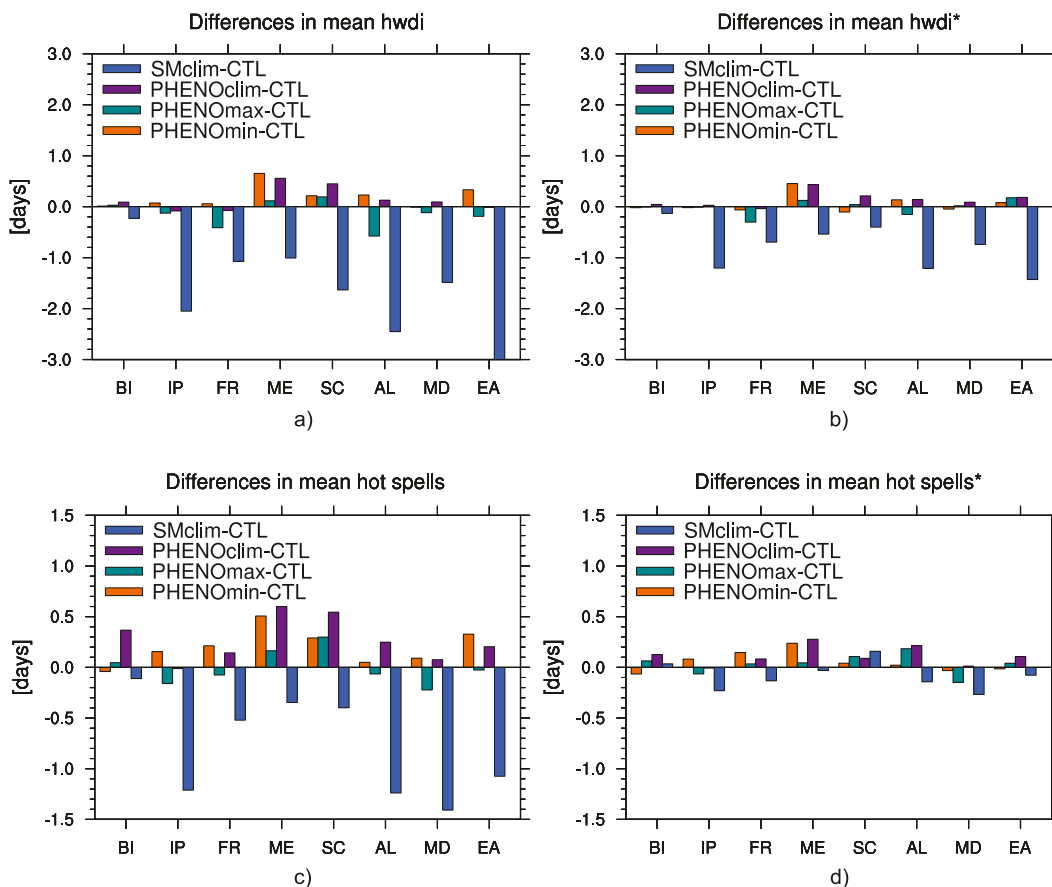
FIG. 7. Differences in mean heat wave indices: (a) hwdi, (b) hwdi[★], (c) hot spells, and (d) hot spells[★].

the amount of soil ice is increased. This leads to an increase in ground heat flux, reducing the available energy for H and λE and therefore reducing evapotranspiration in the (energy limited) northern part of the continent.

4. Effect of LAI and SM changes on temperature extremes

a. Phenology effects on heat wave duration

Figure 7 displays differences to CTL in four heat wave duration indices for PHENO$_{min}$ (orange), PHENO$_{max}$ (turquoise), PHENO$_{clim}$ (violet), and SM$_{clim}$ (blue) for all eight PRUDENCE subdomains. In this section we focus on Figs. 7a and 7c. Even though the differences from CTL for the PHENO$_{min}$ and PHENO$_{max}$ experiments were larger than for PHENO$_{clim}$ for the mean summer climate, the effect of removing interannual variability in LAI has an effect on heat waves that is of a similar order of magnitude as for the maximum and minimum experiments. The two heat wave indices hwdi (Fig. 7a) and hot spells (Fig. 7c) are comparable in their spatial patterns. The duration of the hot spells is

generally shorter than hwdi since they also take into account warm nights in their definition. The general geographical regions of increased and decreased heat wave duration for an experiment are similar for the two heat wave indices. PHENO$_{min}$ exhibits an increase in hwdi and hot spells in all regions. PHENO$_{max}$ shows increasing hwdi and hot spells for northern regions (BI, ME, and SC) and decreasing hwdi and hot spells in all other regions. PHENO$_{clim}$ mostly shows increasing hwdi and hot spells.

However, the patterns are not homogeneous (not shown), which indicates that other effects (e.g., climate conditions or vegetation or soil types) are of similar importance, especially at the local scale. As discussed in section 3b, changes in LAI can have different effects in different regions since several processes (transpiration, ground evaporation, shading of ground and therefore change in available net radiation, etc.) interact and modify one another. Therefore, depending on the geographical region, the effects from phenology on heat waves vary in sign and magnitude. Generally, a higher LAI decreases interannual temperature variability and tends to decrease heat wave lengths. A lower LAI rather increases heat wave length.

b. Phenology versus soil moisture effects on heat waves

To assess the impact of vegetation phenology versus SM on climate we compare prescribed-SM and prescribed-phenology experiments. In the SM experiment (SM_{clim}), SM is prescribed to the seasonal cycle from CTL. The counterpart is $PHENO_{clim}$, where LAI is prescribed to a daily climatological cycle. Since SM is still interactive in $PHENO_{clim}$ whereas LAI is prescribed in SM_{clim}, the two experiments are not totally equivalent. Nevertheless, by comparing the differences between $PHENO_{clim}$ − CTL and SM_{clim} − CTL for temperature extremes we roughly see the difference in vegetation versus SM effects (Fig. 7, violet and blue bars).

For the SM experiment we find a decrease in heat wave duration over almost all of Europe. For $PHENO_{clim}$ Fig. 7 displays regions with increases and regions with decreases. In some regions, all phenology experiments (in which no interannual variability in LAI is present) have enhanced heat wave duration (e.g., ME and SC). This suggests that in these regions the variability in LAI is most important for heat wave duration, and not the actual LAI level. The effects from $PHENO_{clim}$ are smaller compared to SM_{clim}, especially for hwdi. However, the effects on mean summer temperature are smaller for the phenology experiments (see Fig. 6b, with a decrease in mean summer temperature $\geq 0.5°C$ over large areas). This has an influence on the extremes if we calculate heat wave duration with reference to CTL (as shown in Figs. 7a,c). If we look at hwdi[★] and hot spells[★] (Figs. 7b,d) where we take the 90th percentile from SM_{clim} and $PHENO_{clim}$, respectively, we can set aside the impact of mean temperature changes on the spell durations (see also Lorenz et al. 2010). For the phenology experiments the differences between these indices (hwdi and hwdi[★]) are rather small, since the changes in mean summer climate are very small. When we use hwdi[★] and hot spells[★] the effects from the SM and phenology experiment are more comparable in magnitude or even more pronounced for phenology for hot spells[★] in some regions (e.g., ME in Fig. 7d). The effect of prescribing SM to the climatology is alleviating heat waves everywhere except hot spells[★] in BI and SC, whereas the effect of prescribing phenology without interannual variability increases heat wave duration in most regions.

c. Case study: Hot summer 2003 in western and central Europe

During the 2003 summer, Europe experienced a record-breaking hot summer (Schär et al. 2004), which was possibly the hottest of the last 500 years (Luterbacher

et al. 2004). Two main heat waves occurred, the first one in June and the second, even hotter, in August. The main cause for the occurring heat waves was a persistent anti-cyclonic circulation anomaly (e.g., Ferranti and Viterbo 2006; García-Herrera et al. 2010). Several studies have shown that an SM deficit enhanced the hot temperatures in summer 2003, especially during the second heat wave in August (Ferranti and Viterbo 2006; Fischer et al. 2007a,b). It has also been suggested that early vegetation green-up together with a precipitation deficit in spring 2003 played an important role for the heat wave (e.g., Zaitchik et al. 2006; Fischer et al. 2007a,b; Loew et al. 2009). A general analysis of the heat wave characteristics and its representation in the CTL simulation can be found in the appendices.

Figure 8a displays the time series of the anomalies in prescribed LAI (in green) averaged over France. A negative LAI anomaly is seen in summer. However, there is only a very small positive LAI anomaly in spring and early summer, in contrast to the expectations from, for example, Zaitchik et al. (2006), Fischer et al. (2007b), and Loew et al. (2009), who proposed an early vegetation onset. Lafont et al. (2012) found a more contrasted response with above-normal LAI in northwestern France and below-normal LAI in southeastern France in June. We find a positive LAI anomaly over the Alps (and Scandinavia) in June (Fig. B1a) in our data; indicating that some regions experienced more pronounced greening due to the warm spring. However, we do not find distinct positive anomalies in vegetation state during spring in other regions.

Figure 8a also displays the time series of the simulated (CTL) SM and T_{max} anomalies averaged over France. SM was already smaller than normally in spring and this negative anomaly became even more pronounced in summer. The positive temperature anomalies in summer show the timing of the 2003 heat waves, with the distinct heat wave peaks in June and August. In addition to the model results, the temperature anomaly for E-OBS observations is shown in black. Additional maps illustrating the 2003 heat waves and drought are presented in the appendix (Fig. B1). This figure shows anomalies in LAI (Figs. B1a–c), SM (Figs. B1d–f), T_{max} (Figs. B1g–i), λE (Figs. B1j–l), H (Figs. B1m–o), and R_{net} (net radiation; Figs. B1p–r) for June, July, and August 2003 as maps over Europe. Altogether, the development of the 2003 summer in the model simulations is consistent with results from E-OBS observations and the known literature, even if the temperature anomaly is rather underestimated.

To illustrate the influence of vegetation and SM state on the heat waves, Fig. 8a also displays the anomalies in T_{max} for $PHENO_{clim}$ and SM_{clim} and Fig. 8b shows these
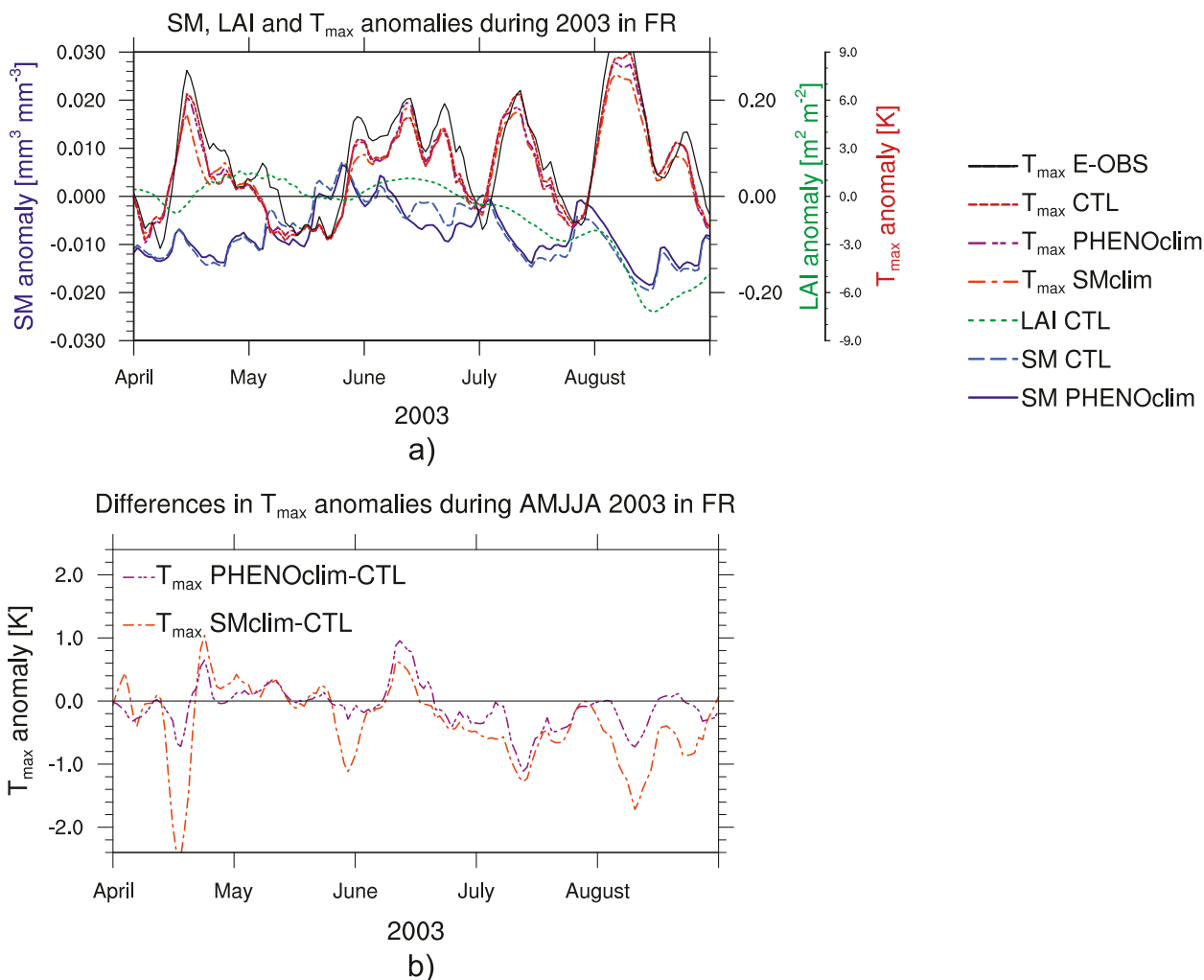
FIG. 8. (a) Anomalies in total leaf area index in CTL, soil moisture in CTL and PHENO$_{clim}$, and daily maximum temperature in CTL, PHENO$_{clim}$, and SM$_{clim}$ and (b) differences in T_{max} anomalies between PHENO$_{clim}$ and CTL and SM$_{clim}$ and CTL during spring and summer 2003 in France.

differences from CTL directly. Additionally, in Fig. 8a the SM anomaly for PHENO$_{clim}$ is shown. Generally, the time evolution of T_{max} is similar in all model runs. Hence, soil moisture and phenology do not influence the main features of the heat waves. However, the largest peak in August is clearly smaller in the runs without variability in phenology and SM, respectively (Fig. 8b). The net effects from phenology and SM feedbacks around the hottest days in August (averaged over 1 week) in France are summarized in Table 3. The heat wave peak is dampened by more than 1°C by climatological SM and almost 0.5°C by climatological LAI. The first extended heat wave in June is amplified by climatological SM as well as climatological LAI. The SM anomaly in PHENO$_{clim}$ is larger than the one in CTL causing the T_{max} peak to be highest for PHENO$_{clim}$ in June.

d. Case study: Hot summer 2007 in southeastern Europe

A similar analysis was carried out for the heat wave that occurred in southeastern Europe during 2007. The 2007 heat wave had large impacts in the affected regions, ranging from excess deaths to power outages and forest fires (Founda and Giannakopoulos 2009; Barriopedro et al. 2011). Figure 9a displays the time series of LAI,

TABLE 3. Differences in T_{max} during heat wave peaks (averaged over 1 week) in 2003 and 2007 between CTL and PHENO$_{clim}$ and CTL and SM$_{clim}$, respectively.

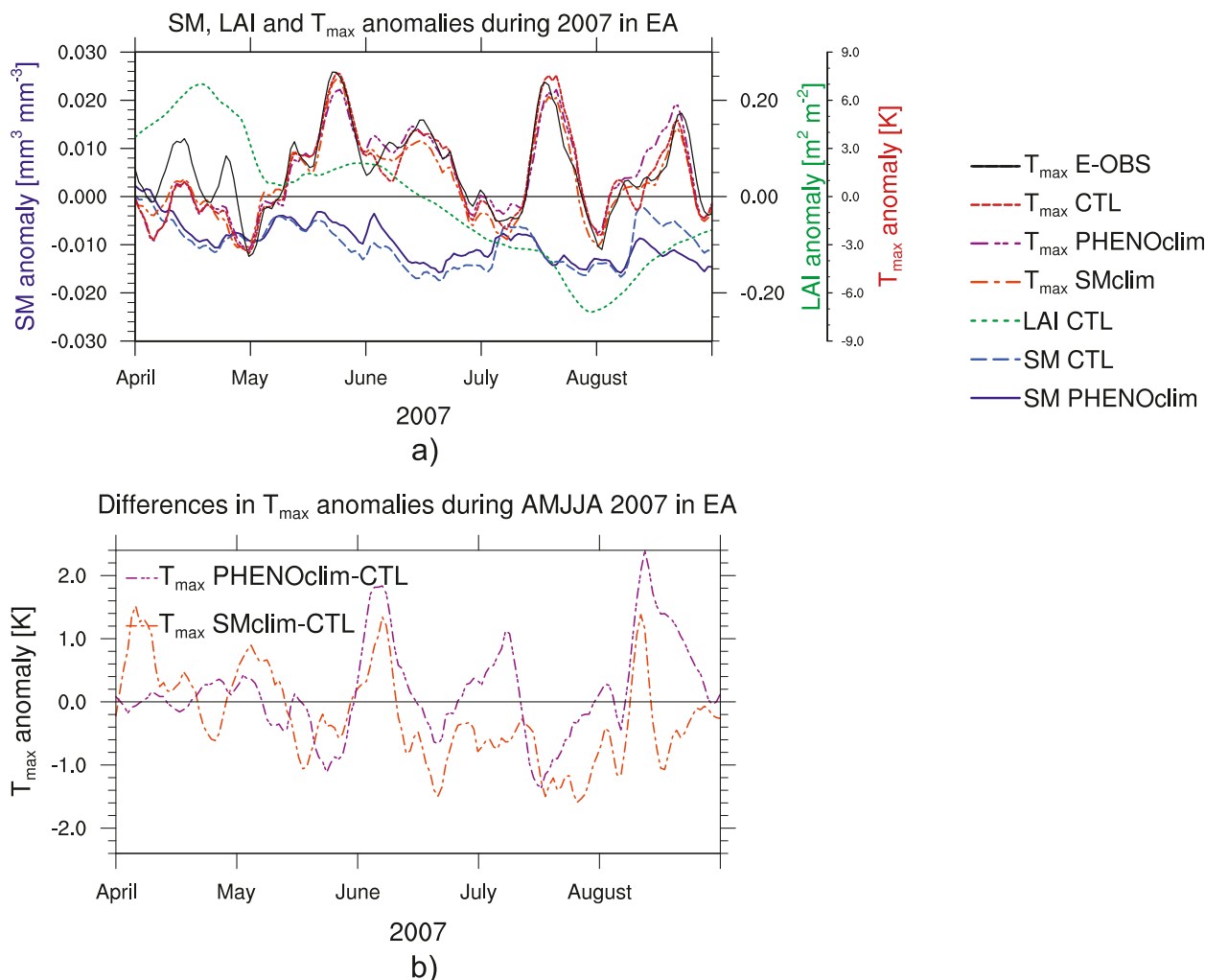| Year	Domain	CTL − PHENO$_{clim}$	CTL − SM$_{clim}$
2003	FR	+0.48	+1.19
2007	EA	+0.65	+1.33

FIG. 9. As in Fig. 8, but during spring and summer 2007 in eastern Europe.

SM, and T_{max} over eastern Europe during 2007, including the temperature anomaly from E-OBS observations. Generally, the temperature anomaly compares well with the observed values. However, the positive temperature anomaly in April is not well captured in the model runs. In the appendix (Fig. B2), the associated anomalies during summer 2007 for LAI, SM, T_{max}, λE, H, and R_{net} are provided as maps over Europe. The affected region was restricted to southeastern Europe where a large negative anomaly in soil moisture persisted during the whole summer. The negative soil moisture anomaly was caused by pronounced negative precipitation anomalies during winter 2007 over the entire Mediterranean (e.g., Luterbacher et al. 2007). In contrast to the 2003 event, the 2007 event starts with a pronounced positive LAI anomaly in spring. A negative LAI anomaly established over July and August. Note also that the region affected by the 2007 heat wave overlaps with the region where the interannual variability in LAI is among the largest in our dataset. This area is, therefore, expected to be more affected by phenology feedbacks than the rest of Europe.

Again we display the anomalies in T_{max} for PHENO$_{clim}$ and SM$_{clim}$, and the SM anomaly for PHENO$_{clim}$ in addition to CTL. At the heat wave peak in July we see the same effect as for the 2003 heat waves, a dampening of the peak for PHENO$_{clim}$ and SM$_{clim}$. Figure 9b and Table 3 reveal that LAI dampens the heat wave by more than 0.5°C and SM by more than 1°C. Hence, the dampening of the heat wave peak from applying climatological LAI is about half that resulting from prescribing climatological SM. However, the smaller heat wave peak in August is higher in PHENO$_{clim}$ than CTL. In this case also the duration of the positive T_{max} anomaly is modified by the experiments. If we take SM into account as well, we see that the SM anomaly in PHENO$_{clim}$ is even more

pronounced than in the reference run in August. Hence, the cause for the enhanced T_{max} in PHENO$_{clim}$ in August is due to SM–temperature feedbacks. The fact that LAI does not decrease in PHENO$_{clim}$ leads to a stronger SM depletion compared to experiment CTL, thereby further amplifying the heat wave. Thus, the 2007 case confirms that phenology effects can either dampen or amplify heat waves. Their overall sign depends on whether the SM depletion effect or the transpiration reduction effect is dominant.

5. Discussion and conclusions

In this study we performed RCM experiments to investigate impacts of phenology on climate and compare their magnitude to that of soil moisture–climate feedbacks. Our results suggest that today's European mean spring and summer climate is not strongly affected by vegetation phenology, although we note that the employed model might have a tendency to underestimate phenological effects on climate due to an overly large compensation effect between transpiration and ground evaporation.

Specifically, the simulated effects from phenology on mean summer climate are much smaller than those from SM. Since variability in LAI is not very pronounced over Europe, effects may be larger in regions where the LAI variability is more extreme (Bounoua et al. 2000; Lawrence and Slingo 2004; Rechid and Jacob 2006). Additionally, model structural biases, such as low soil moisture variability (Oleson et al. 2008) or total soil moisture or evapotranspiration partitioning (Lawrence and Chase 2009), could affect the sensitivity of the model in our experiments. Levis and Bonan (2004) have shown a relatively strong impact on springtime warming rates from the timing of leaf emergence using an earlier version of the Community Land Model (CLM2). CLM2 was drier on average than the version used here, which possibly caused the larger response to LAI. In particular, the large compensation of changes in transpiration by ground evaporation is questionable (Lawrence and Chase 2009; Boisier et al. 2012) in the present version. Hence, the influence of vegetation phenology on climate could be larger in reality than in the model we used.

The effects of phenology in the context of climate extremes, however, are found to be important. We found that effects on heat wave duration are of the same order of magnitude for phenology and SM, if we do not take into account the larger effect on mean summer climate in the case of SM. The climatological state of LAI has rather amplifying effects on heat wave duration. In general, late and weak greening has amplifying effects on heat waves and early and strong greening has dampening effects; however, the effects from strong greening depend largely on the considered region.

In the case of the 2003 summer, the model simulations are largely consistent with results from other studies. However, our dataset does not show early greening of the vegetation over large areas as shown by Zaitchik et al. (2006) for France and proposed by Fischer et al. (2007b). We only find positive anomalies in LAI over Scandinavia and the Alps in early summer 2003. This is consistent with the findings of Jolly et al. (2005). Phenology effects did nonetheless play a role during 2003, as our dataset shows a pronounced decrease in LAI during this hot summer. We could show that the decrease in LAI further increased maximum temperatures during July and August in France. Stefanon et al. (2012) investigated interactive vegetation phenology in 2003 and found a dampening effect in the June heat wave and an amplifying effect of interactive vegetation in the August heat wave. Our results confirm this finding. Hence, phenology amplified the 2003 event by about 0.5°C during the hottest period in August, but did not initiate it. We also analyzed the heat wave occurring in southeastern Europe during summer 2007. The results for this event confirm the findings for the 2003 case study that heat waves can be amplified by phenology impacts. However, they also show that anomalies in LAI can dampen heat waves if reduced LAI prevents SM depletion. However, whereas the dampening in June 2003 results from anomalously high evapotranspiration due to high insolation and slightly higher LAI, in August 2007 the effect that a decreased LAI prevents transpiration and, therefore, more SM stays in the soil than in the case with climatological LAI plays a major role. The 2007 case illustrates clearly that in regions with large LAI variability, phenology plays an important role for extreme temperature events. Hence, in some cases enhanced temperature during heat waves can be caused by phenology effects and drought conditions, whereas we find that the effects from vegetation phenology generally are about half as large, and sometimes even as large, as those from soil moisture.

However, the sensitivity of the model used is small to the applied experiments and the results are dependent on the model structure. In reality the influence of vegetation phenology on climate could be larger. Therefore, we would like to see similar experiments to be repeated in other modeling systems to investigate the influence of the model structure on model sensitivity to vegetation phenology. In addition, including interactive calculation of vegetation dynamics and the carbon cycle could reveal interesting results. We did not investigate the sensitivity of carbon fluxes during heat waves and droughts to phenology. The sensitivity of the carbon fluxes might be much larger since phenology and soil moisture effects amplify one another for carbon, in contrast to the water fluxes for which effects of phenology and soil moisture on transpiration and ground evaporation dampen one another.
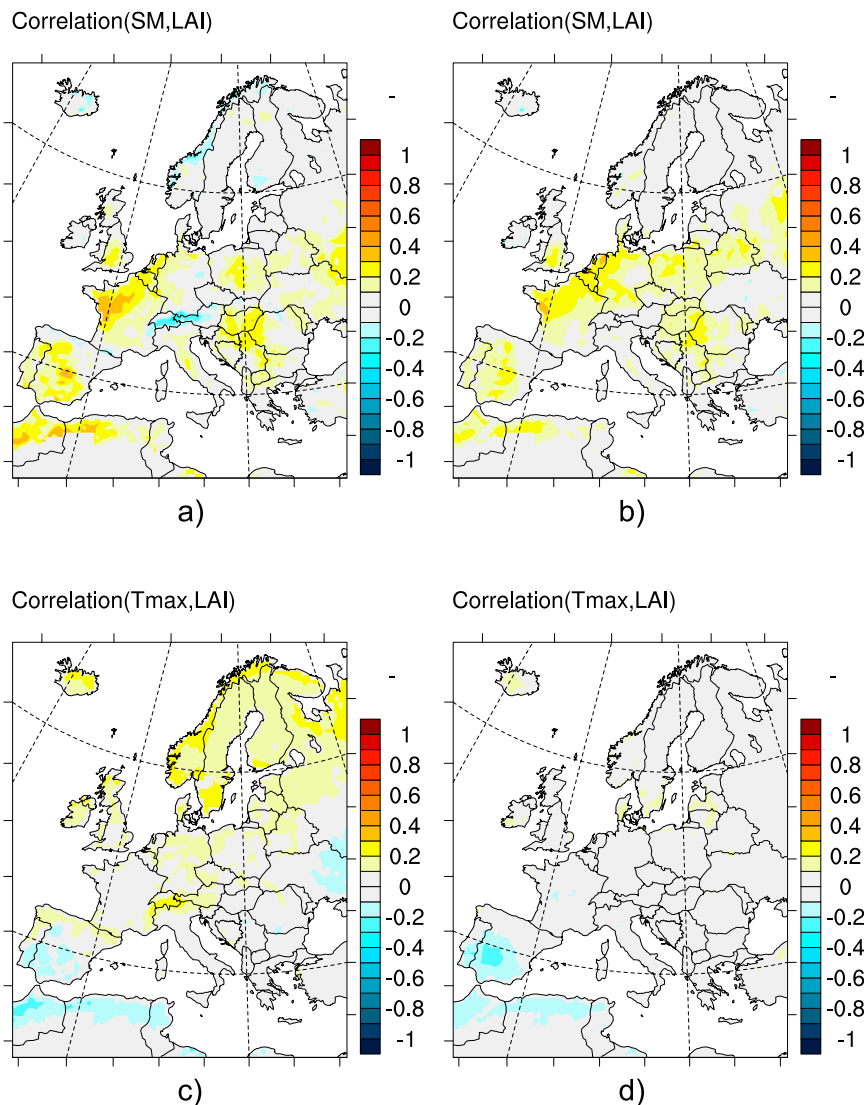
Correlation(SM,LAI)   Correlation(SM,LAI)

a)   b)

Correlation(Tmax,LAI)   Correlation(Tmax,LAI)

c)   d)

FIG. A1. (a),(b) Lag correlation for SM and LAI for (left) lag 0 and (right) lag 30. (c),(d) Lag correlation for T_{max} and LAI for the same lags.

APPENDIX A

Evaluation of LAI Data within Models

a. Correlation maps

This appendix displays lag correlations between SM and LAI as well as T_{max} and LAI to ensure that the
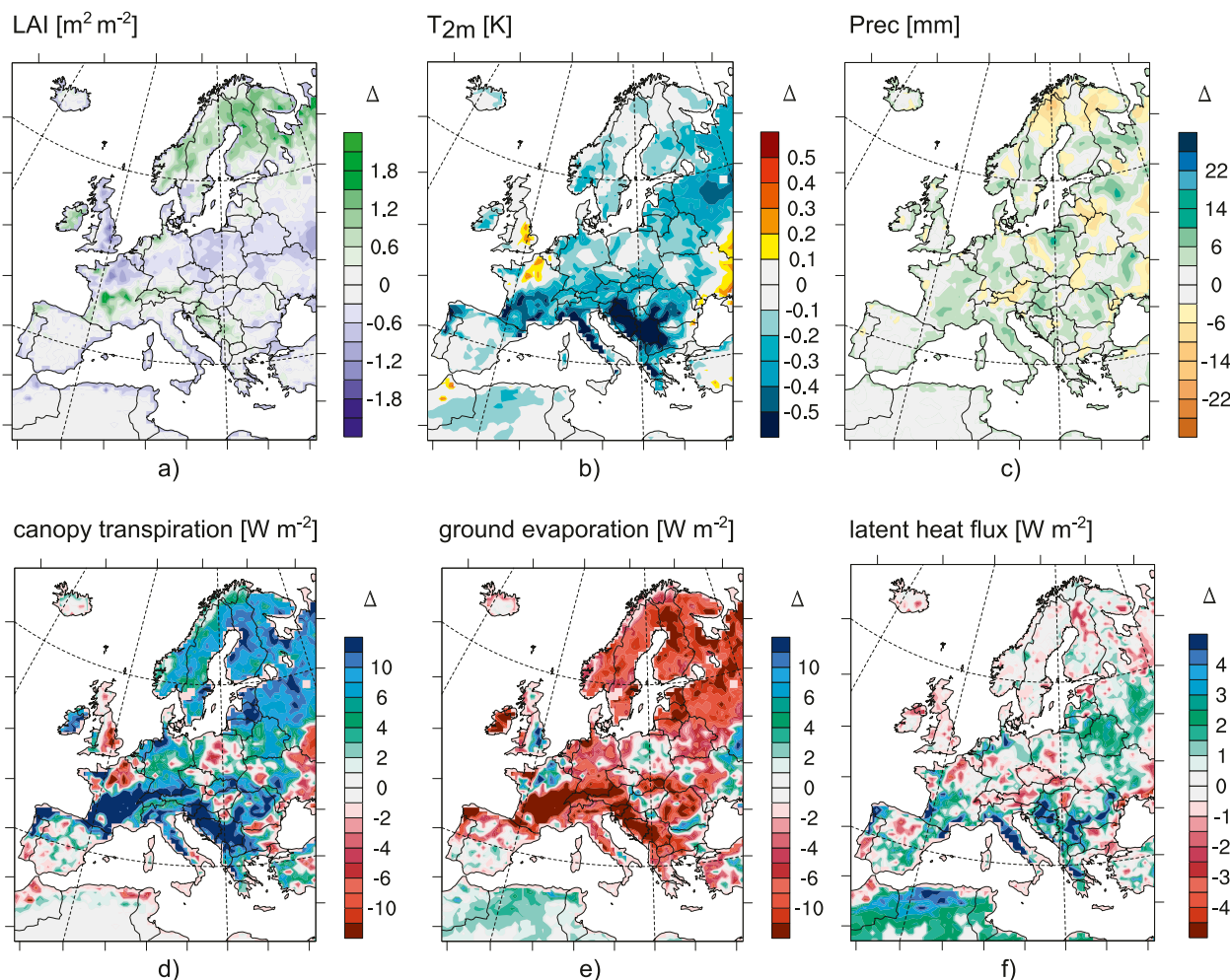
FIG. A2. Differences in mean summer (a) LAI, (b) temperature (at 2 m), (c) precipitation, (d) canopy transpiration, (e) ground evaporation, and (f) latent heat flux for $PHENO_{old}$ − CTL.

prescribed LAI corresponds to the simulated soil moisture and temperatures. We could verify the positive correlation between SM and LAI (since plants rely on SM for growth) between our LAI dataset and the SM model output (Figs. A1a,b). The correlation between T_{max} anomalies and LAI anomalies is positive in northern Europe, some regions in central Europe, northern Spain, and the Alps (Figs. A1c,d). In contrast, the correlation is slightly negative in southern Europe. This is reasonable since warm temperatures favor plant growth in central and northern Europe but excessively high temperatures can have long-term negative effects in the drier south.

b. CTL versus $PHENO_{old}$

Figure A2 shows differences in mean summer temperature between $PHENO_{old}$ (older run with default monthly LAI dataset) and CTL (new daily LAI dataset).

The distribution in plant functional types is not changed between these two model simulations, only the LAI dataset. Central Europe shows mainly smaller LAI in $PHENO_{old}$ whereas there are higher LAI values in Scandinavia, southern France, the Alpine region, and the Balkans in $PHENO_{old}$ (Fig. A2a). The main difference in temperature is a lower temperature in $PHENO_{old}$ by up to 0.5°C (Fig. A2b), which goes along with mainly higher precipitation (Fig. A2c). Figures A2d–f display the evapotranspiration-related variables. Transpiration (Fig. A2d) is mainly higher in $PHENO_{old}$ whereas ground evaporation (Fig. A2e) is mainly higher in CTL. The resulting difference in λE (Fig. A2f) is rather small; $PHENO_{old}$ shows generally higher values especially in the south, corresponding well with the difference in T_{2m}. Thus, the effects from the higher LAI values in $PHENO_{old}$ dominate, resulting in increased λE and decreased temperature.
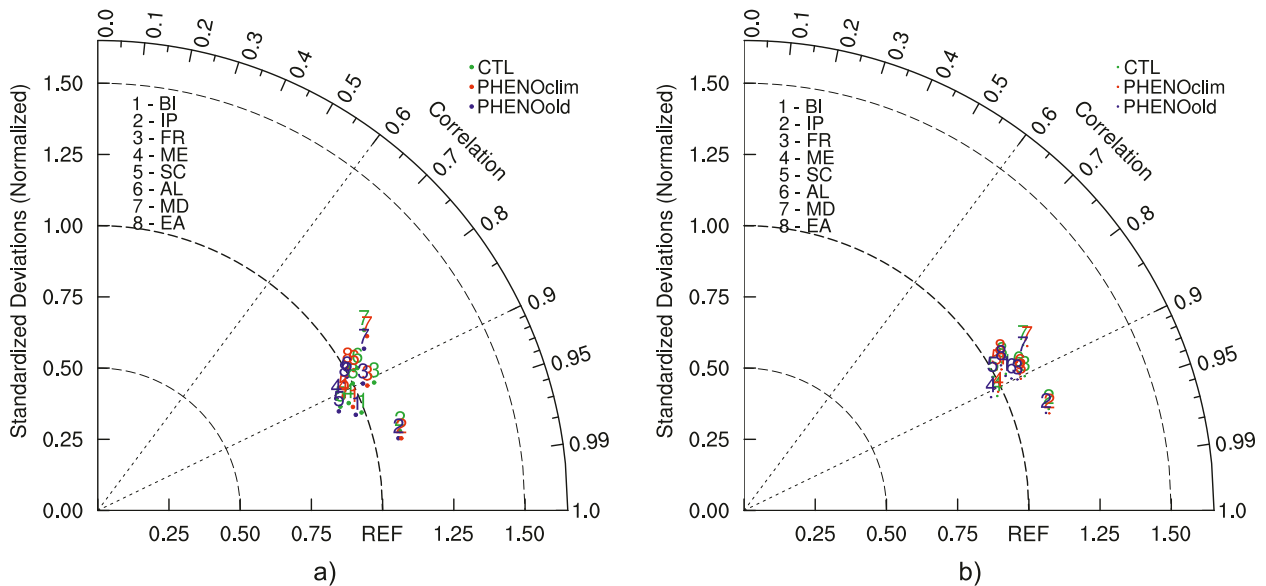
FIG. A3. Taylor diagrams for (a) monthly and (b) daily temperature data in PHENO$_{old}$, CTL, and PHENO$_{clim}$ for all PRUDENCE domains.

Even though we obtain an increase in T_{2m} of up to 0.5°C with the new LAI dataset, the overall performance compared to observations is not very much influenced. The standard deviation and correlation are about 0.75–1.25 and 0.9 in PHENO$_{old}$, CTL as well as PHENO$_{clim}$ for daily and monthly summer temperature values (Fig. A3).

APPENDIX B

Additional Maps for 2003 and 2007 Case Studies

a. 2003 drought and heat waves

Figure B1 shows anomalies in summer 2003 as maps over Europe. Figures B1a–c show the development of the pronounced negative LAI anomaly in the area of the heat waves (T_{max} anomalies in Figs. B1g–i). Figures B1d–f show the associated negative soil moisture anomaly. The main cause for the occurring heat waves was a persistent anticyclonic circulation anomaly (e.g., Ferranti and Viterbo 2006; García-Herrera et al. 2010). Our model results confirm the associated positive anomalies in net radiation due to the above-average incoming shortwave radiation and clear skies (Figs. B1p–r). Already in spring, we found anomalous high net radiation and associated temperatures, and below-average precipitation and negative anomalies in SM. Latent heat flux was higher than usual already in spring over large areas in Europe (Fig. B1j). These conditions were even more pronounced in summer, especially in France and central Europe,

leading to further decreased SM (Fig. B1f). In June, the positive anomaly in λE was higher than in August in France and central Europe (Figs. B1j,l), mainly due to above-average transpiration (not shown). In August the positive anomaly in transpiration and thus λE decreased. The anomaly in H was negative in June over France and central Europe (Fig. B1m). Total H was positive, but because warm air was advected from the large-scale circulation, the air was warmer than the surface. So, hot air was warming the ground more strongly than under normal conditions. In August, the regions where we found a positive anomaly in H were more extended (Fig. B1o). This confirms that the additional energy provided by the high incoming radiation was less balanced by latent heat flux; instead, sensible heat flux was increased even further in late summer. The region with the strongest T_{max} anomalies in August 2003 only partially overlaps with the region with the highest net radiation (Fig. B1r). But in France, where the second phase of the 2003 heat wave was strongest, we find a pronounced decrease in LAI and SM compared to the climatology. This indicates a strengthening effect of the land surface on maximum temperatures in this region during the 2003 summer. Altogether, summer 2003 was represented in the model run in agreement with previous studies.

b. 2007 heat wave

Figure B2 displays anomalies in summer 2007 as maps over Europe. The first two rows show the associated
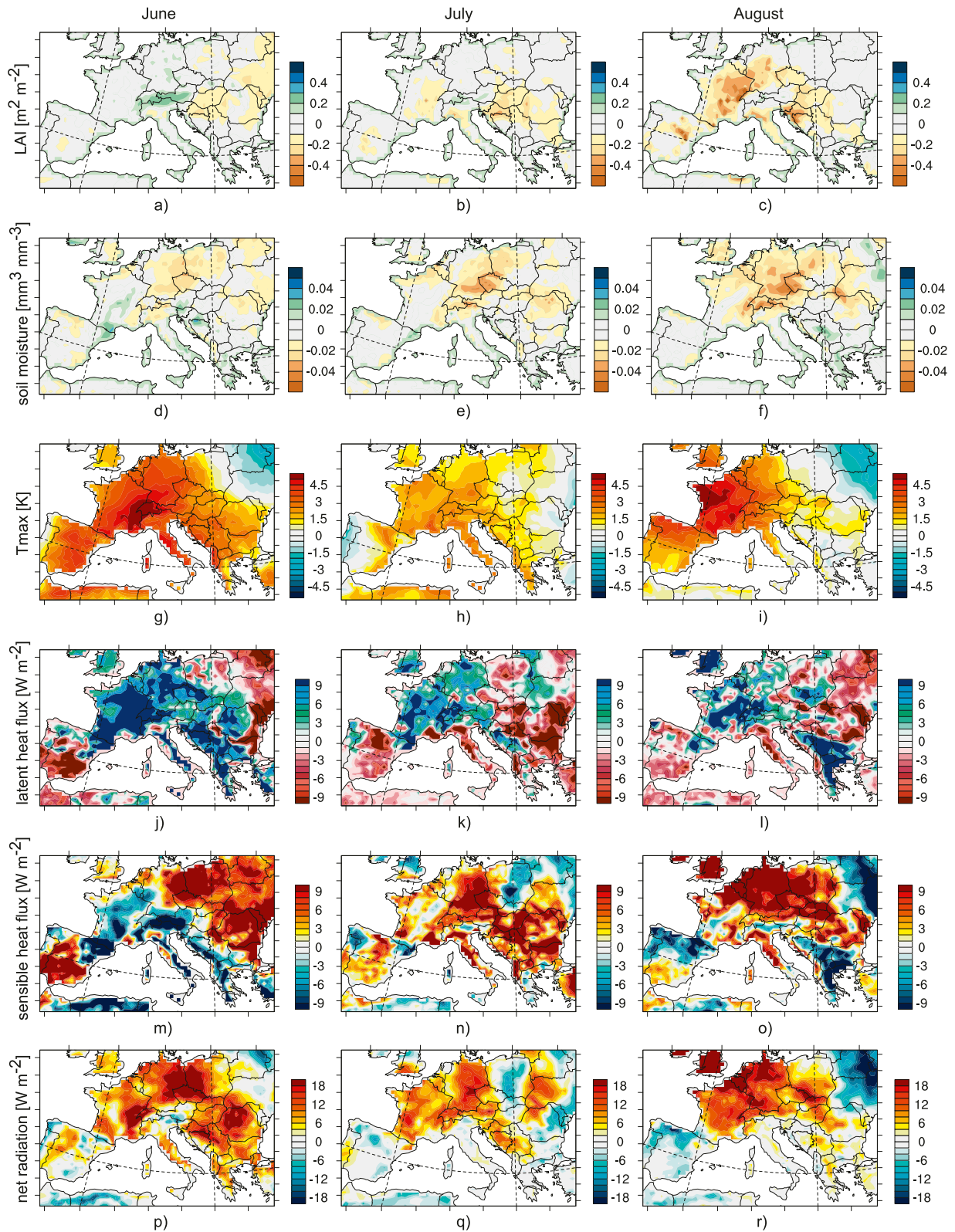
FIG. B1. Anomalies in (a)–(c) total leaf area index, (d)–(f) soil moisture, (g)–(i) daily maximum temperature, (j)–(l) latent heat flux, (m)–(o) sensible heat flux, and (p)–(r) net radiation in CTL during (left) June, (center) July, and (right) August 2003.
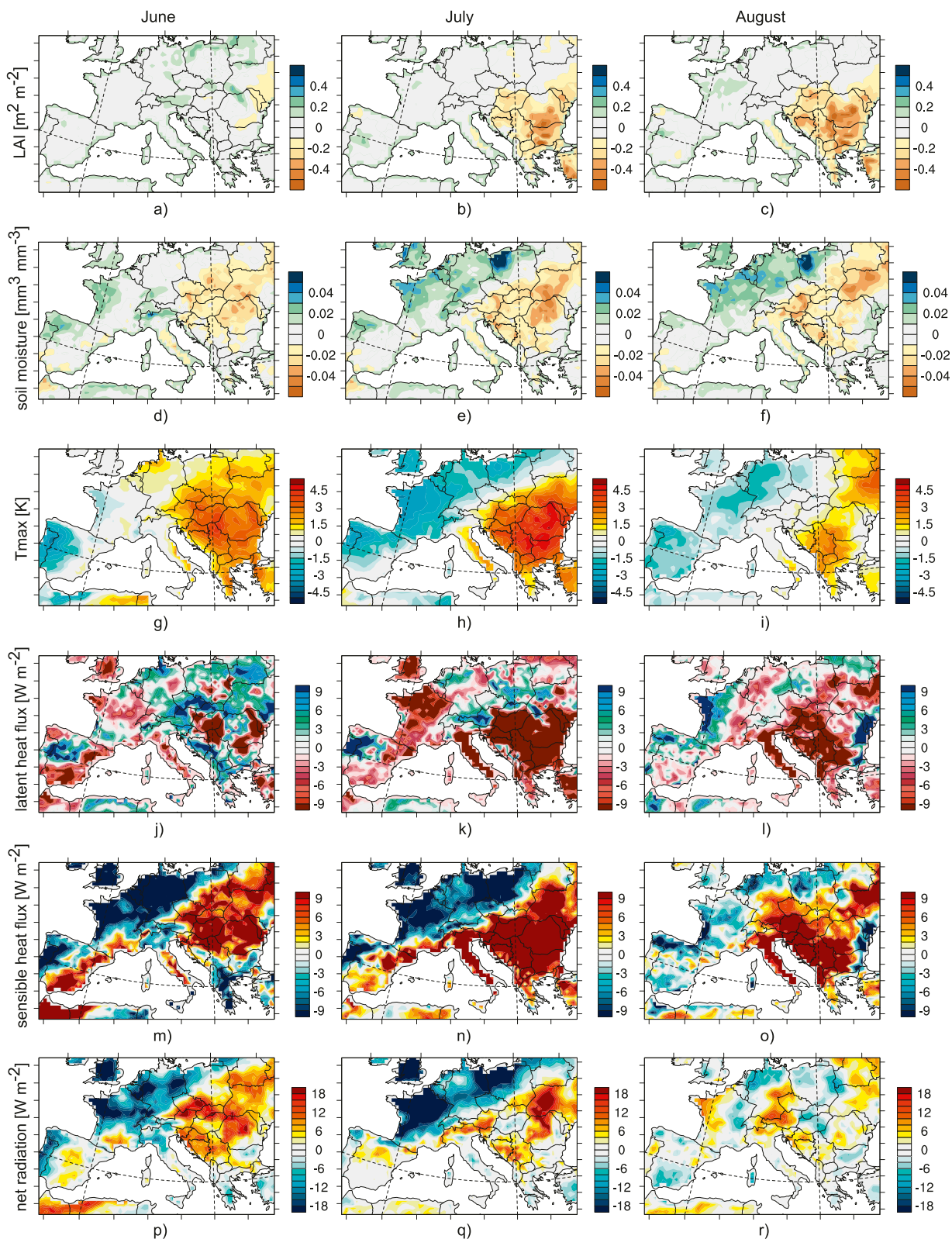
FIG. B2. As in Fig. B1, but for 2007.

decrease in LAI and SM over summer. Figures B2g–i show the hot temperature anomalies in southeastern Europe. The latent heat flux exhibited a positive anomaly at the beginning of summer but then this anomaly became negative over most of Europe by August (Figs. B2 j–l). In contrast, the positive anomaly in sensible heat flux increased in both magnitude and geographical extent during summer, confirming a change in the partitioning of the energy fluxes caused by the land surface conditions. The resulting positive temperature anomalies are a combined result of soil moisture–temperature and phenology–temperature feedbacks. The shift from positive λE anomalies to negative λE anomalies, and vice versa for H, agrees well with the results of Teuling et al. (2010) for heat waves over grassland in Europe.

REFERENCES

Arneth, A., and Coauthors, 2010: Terrestrial biogeochemical feedbacks in the climate system. *Nat. Geosci.,* **3,** 525–532, doi:10.1038/ngeo905.

Arora, V. K., 2002: Modeling vegetation as a dynamic component in soil–vegetation–atmosphere transfer schemes and hydrological models. *Rev. Geophys.,* **40,** 1006, doi:10.1029/2001RG000103.

Barriopedro, D., E. M. Fischer, J. Luterbacher, R. M. Trigo, and R. García-Herrera, 2011: The hot summer of 2010: Redrawing the temperature record map of Europe. *Science,* **332,** 220–224, doi:10.1126/science.1201224.

Betts, R. A., 2004: Understanding hydrometeorology using global models. *Bull. Amer. Meteor. Soc.,* **85,** 1673–1688.

——, P. D. Falloon, K. K. Goldewijk, and N. Ramankutty, 2007: Biogeophysical effects of land use on climate: Model simulations of radiative forcing and large-scale temperature change. *Agric. For. Meteor.,* **142,** 216–233, doi:10.1016/j.agrformet.2006.08.021.

Boisier, J. P., and Coauthors, 2012: Attributing the impacts of land-cover changes in temperate regions on surface temperature and heat fluxes to specific causes: Results from the first LUCID set of simulations. *J. Geophys. Res.,* **117,** D12116, doi:10.1029/2011JD017106.

Bonan, G. B., 2008: *Ecological Climatology: Concepts and Applications.* 2nd ed. Cambridge University Press, 550 pp.

Bounoua, L., G. J. Collatz, S. O. Los, P. J. Sellers, D. A. Dazlich, C. J. Tucker, and D. A. Randall, 2000: Sensitivity of climate to changes in NDVI. *J. Climate,* **13,** 2277–2292.

Boussetta, S., G. Balsamo, A. Beljaars, T. Kral, and L. Jarlan, 2012: Impact of a satellite-derived leaf area index monthly climatology in a global numerical weather prediction model. *Int. J. Remote Sens.,* **34**, 3520–3542, doi:10.1080/01431161.2012.716543.

Buermann, W., J. Dong, X. Zeng, R. B. Myneni, and R. E. Dickinson, 2001: Evaluation of the utility of satellite-based vegetation leaf area index data for climate simulations. *J. Climate,* **14,** 3536–3550.

Christensen, J. H., and O. B. Christensen, 2007: A summary of the PRUDENCE model projections of changes in European climate by the end of this century. *Climatic Change,* **81,** 7–30, doi:10.1007/s10584-006-9210-7.

Davin, E. L., and N. de Noblet-Ducoudré, 2010: Climatic impact of global-scale deforestation: Radiative versus nonradiative processes. *J. Climate,* **23,** 97–112.

——, and S. I. Seneviratne, 2012: Role of land surface processes and diffuse/direct radiation partitioning in simulating the European climate. *Biogeosciences,* **9,** 1695–1707, doi:10.5194/bg-9-1695-2012.

——, R. Stöckli, E. B. Jaeger, S. Levis, and S. I. Seneviratne, 2011: COSMO-CLM^2: A new version of the COSMO-CLM model coupled to the Community Land Model. *Climate Dyn.,* **37,** 1889–1907, doi:10.1007/s00382-011-1019-z.

Dee, D. P., and Coauthors, 2011: The ERA-Interim reanalysis: Configuration and performance of the data assimilation system. *Quart. J. Roy. Meteor. Soc.,* **137,** 553–597, doi:10.1002/qj.828.

de Noblet-Ducoudré, N., and Coauthors, 2012: Determining robust impacts of land-use-induced land cover changes on surface climate over North America and Eurasia: Results from the first set of LUCID experiments. *J. Climate,* **25,** 3261–3281.

Ferranti, L., and P. Viterbo, 2006: The European summer of 2003: Sensitivity to soil water initial conditions. *J. Climate,* **19,** 3659–3680.

Fischer, E. M., S. I. Seneviratne, D. Lüthi, and C. Schär, 2007a: Contribution of land–atmosphere coupling to recent European summer heat waves. *Geophys. Res. Lett.,* **34,** L06707, doi:10.1029/2006GL029068.

——, ——, P. L. Vidale, D. Lüthi, and C. Schär, 2007b: Soil moisture–atmosphere interactions during the 2003 European summer heat wave. *J. Climate,* **20,** 5081–5099.

Founda, D., and C. Giannakopoulos, 2009: The exceptionally hot summer of 2007 in Athens, Greece—A typical summer in the future climate? *Global Planet. Change,* **67,** 227–236, doi:10.1016/j.gloplacha.2009.03.013.

García-Herrera, R., J. Díaz, R. M. Trigo, J. Luterbacher, and E. M. Fischer, 2010: A review of the European summer heat wave of 2003. *Crit. Rev. Environ. Sci. Technol.,* **40,** 276–306, doi:10.1080/10643380802238137.

Guillevic, P., R. D. Koster, M. J. Suarez, L. Bounoua, G. J. Collatz, S. O. Los, and S. P. P. Mahanama, 2002: Influence of the interannual variability of vegetation on the surface energy balance—A global sensitivity study. *J. Hydrometeor.,* **3,** 617–629.

Haylock, M. R., N. Hofstra, A. M. G. Klein Tank, E. J. Klok, P. D. Jones, and M. New, 2008: A European daily high-resolution gridded data set of surface temperature and precipitation for 1950–2006. *J. Geophys. Res.,* **113,** D20119, doi:10.1029/2008JD010201.

Jaeger, E. B., and S. I. Seneviratne, 2011: Impact of soil moisture–atmosphere coupling on European climate extremes and trends in a regional climate model. *Climate Dyn.,* **36,** 1919–1939, doi:10.1007/s00382-010-0780-8.

Jeong, S.-J., C.-H. Ho, T.-W. Park, J. Kim, and S. Levis, 2011: Impact of vegetation feedback on the temperature and its diurnal range over the Northern Hemisphere during summer in a 2x CO_2 climate. *Climate Dyn.,* **37,** 821–833, doi:10.1007/s00382-010-0827-x.

Jolly, W. M., M. Dobbertin, N. E. Zimmermann, and M. Reichstein, 2005: Divergent vegetation growth responses to the 2003 heat wave in the Swiss Alps. *Geophys. Res. Lett.,* **32,** L18409, doi:10.1029/2005GL023252.

Katul, G. G., R. Oren, S. Manzoni, C. Higgins, and M. B. Parlange, 2012: Evapotranspiration: A process driving mass transport and energy exchange in the soil–plant–atmosphere–climate system. *Rev. Geophys.,* **50,** RG3002, doi:10.1029/2011RG000366.

Koster, R. D., and Coauthors, 2004: Regions of strong coupling between soil moisture and precipitation. *Science,* **305,** 1138–1140.

Lafont, S., Y. Zhao, J. C. Calvet, P. Peylin, P. Cias, F. Maignan, and M. Weiss, 2012: Modelling LAI, surface water and carbon fluxes at high resolution over France: Comparison of ISBA-A-gs and ORCHIDEE. *Biogeosciences,* **9,** 439–456, doi:10.5194/bg-9-439-2012.

Lawrence, D. M., and J. M. Slingo, 2004: An annual cycle of vegetation in a GCM. Part II: Global impacts on climate and hydrology. *Climate Dyn.,* **22,** 107–122, doi:10.1007/s00382-003-0367-8.

——, and Coauthors, 2011: Parameterization improvements and functional and structural advances in version 4 of the Community Land Model. *J. Adv. Model. Earth Syst.,* **3,** M03001, doi:10.1029/2011MS000045.

Lawrence, P. J., and T. N. Chase, 2007: Representing a new MODIS consistent land surface in the Community Land Model (CLM 3.0). *J. Geophys. Res.,* **112,** G01023, doi:10.1029/2006JG000168.

——, and ——, 2009: Climate impacts of making evapotranspiration in the Community Land Model (CLM3) consistent with the Simple Biosphere Model (SiB). *J. Hydrometeor.,* **10,** 374–394.

Levis, S., and G. B. Bonan, 2004: Simulating springtime temperature patterns in the Community Atmosphere Model coupled to the Community Land Model using prognostic leaf area. *J. Climate,* **17,** 4531–4540.

Liu, Z., M. Notaro, and R. Gallimore, 2010: Indirect vegetation–soil moisture feedback with application to Holocene North Africa climate. *Global Change Biol.,* **16,** 1733–1743, doi:10.1111/j.1365-2486.2009.02087.x.

Loew, A., T. Holmes, and R. de Jeu, 2009: The European heat wave 2003: Early indicators from multisensoral microwave remote sensing? *J. Geophys. Res.,* **114,** D05103, doi:10.1029/2008JD010533.

Lorenz, R., E. B. Jaeger, and S. I. Seneviratne, 2010: Persistence of heat waves and its link to soil moisture memory. *Geophys. Res. Lett.,* **37,** L09703, doi:10.1029/2010GL042764.

——, E. L. Davin, and S. I. Seneviratne, 2012: Modeling land–climate coupling in Europe: Impact of land surface representation on climate variability and extremes. *J. Geophys. Res.,* **117,** D20109, doi:10.1029/2012JD017755.

Luterbacher, J., D. Dietrich, E. Xoplaki, M. Grosjean, and H. Wanner, 2004: European seasonal and annual temperature variability, trends, and extremes since 1500. *Science,* **303,** 1499–1503, doi:10.1126/science.1093877.

——, M. A. Liniger, A. Menzel, N. Estrella, P. M. Della-Marta, C. Pfister, T. Rutishauser, and E. Xoplaki, 2007: Exceptional European warmth of autumn 2006 and winter 2007: Historical context, the underlying dynamics, and its phenological impacts. *Geophys. Res. Lett.,* **34,** L12704, doi:10.1029/2007GL029951.

Mellor, G. L., and T. Yamada, 1974: A hierarchy of turbulence closure models for planetary boundary layers. *J. Atmos. Sci.,* **31,** 1791–1806.

——, and ——, 1982: Development of a turbulence closure model for geophysical fluid problems. *Rev. Geophys. Space Phys.,* **20,** 851–875.

Notaro, M., Y. Wang, Z. Liu, R. Gallimore, and S. Levis, 2008: Combined statistical and dynamical assessment of simulated vegetation–rainfall interactions in North Africa during the mid-Holocene. *Global Change Biol.,* **14,** 347–368, doi:10.1111/j.1365-2486.2007.01495.x.

Oleson, K. W., and Coauthors, 2008: Improvements to the Community Land Model and their impact on the hydrological cycle. *J. Geophys. Res.,* **113,** G01021, doi:10.1029/2007JG000563.

Perkins, S. E., L. V. Alexander, and J. R. Nairn, 2012: Increasing frequency, intensity and duration of observed global heatwaves and warm spells. *Geophys. Res. Lett.,* **39,** L20714, doi:10.1029/2012GL053361.

Pielke, S. R. A., R. Avissar, M. Raupach, A. J. Dolman, X. Zeng, and A. S. Denning, 1998: Interactions between the atmosphere and terrestrial ecosystems: Influence on weather and climate. *Global Change Biol.,* **4,** 461–475.

Pitman, A. J., and Coauthors, 2009: Uncertainties in climate responses to past land cover change: First results from the LUCID intercomparison study. *Geophys. Res. Lett.,* **36,** L14814, doi:10.1029/2009GL039076.

Rechid, D., and D. Jacob, 2006: Influence of monthly varying vegetation on the simulated climate in Europe. *Meteor. Z.,* **15,** 99–116, doi:10.1127/0941-2948/2006/0091.

Rockel, B., A. Will, and A. Hense, 2008: The regional climate model COSMO-CLM (CCLM). *Meteor. Z.,* **17,** 347–348, doi:10.1127/0941-2948/2008/0309.

Schär, C., P. L. Vidale, D. Lüthi, C. Frei, C. Häberli, M. A. Liniger, and C. Appenzeller, 2004: The role of increasing temperature variability in European summer heatwaves. *Nature,* **427,** 332–336, doi:10.1038/nature02300.

Sellers, P. J., and Coauthors, 1997: Modeling the exchanges of energy, water, and carbon between continents and the atmosphere. *Science,* **275,** 502–509.

Seneviratne, S. I., D. Lüthi, M. Litschi, and C. Schär, 2006: Land–atmosphere coupling and climate change in Europe. *Nature,* **443,** 205–209.

——, T. Corti, E. L. Davin, M. Hirschi, E. B. Jaeger, I. Lehner, B. Orlowsky, and A. J. Teuling, 2010: Investigating soil moisture-climate interactions in a changing climate: A review. *Earth Sci. Rev.,* **99,** 125–161, doi:10.1016/j.earscirev.2010.02.004.

Stefanon, M., P. Drobinski, F. D'Andrea, and N. de Noblet-Ducoudré, 2012: Effects of interactive vegetation phenology on the 2003 summer heat waves. *J. Geophys. Res.,* **117,** D24103, doi:10.1029/2012JD018187.

Stöckli, R., and P. L. Vidale, 2004: European plant phenology and climate as seen in a 20-year AVHRR land-surface parameter dataset. *Int. J. Remote Sens.,* **25,** 3303–3330, doi:10.1080/01431160310001618149.

——, T. Rutishauser, I. Baker, M. A. Liniger, and A. S. Denning, 2011: A global reanalysis of vegetation phenology. *J. Geophys. Res.,* **116,** G03020, doi:10.1029/2010JG001545.

Teuling, A. J., and Coauthors, 2010: Contrasting response of European forest and grassland energy exchange to heatwaves. *Nat. Geosci.,* **3,** 722–727, doi:10.1038/ngeo950.

Tiedtke, M., 1989: A comprehensive mass flux scheme for cumulus parametrization in large-scale models. *Mon. Wea. Rev.,* **117,** 1779–1800.

Wang, K., and R. E. Dickinson, 2012: A review of global terrestrial evapotranspiration: Observation, modeling, climatology, and climatic variability. *Rev. Geophys.,* **50,** RG2005, doi:10.1029/2011RG000373.

Weiss, M., B. van den Hurk, R. Haarsma, and W. Hazeleger, 2012: Impact of vegetation variability on potential predictability and skill of EC-Earth simulations. *Climate Dyn.,* **39,** 2733–2746, doi:10.1007/s00382-012-1572-0.

Zaitchik, B. F., A. K. Macalady, L. R. Bonneau, and R. B. Smith, 2006: Europe's 2003 heat wave: A satellite view of impacts and

land–atmosphere feedbacks. *Int. J. Climatol.,* **26,** 743–769, doi:10.1002/joc.1280.

Zhang, J., W.-C. Wang, and L. Wu, 2009: Land–atmosphere coupling and diurnal temperature range over the contiguous United States. *Geophys. Res. Lett.,* **36,** L06706, doi:10.1029/2009GL037505.

Zhou, L., R. E. Dickinson, Y. Tian, R. S. Vose, and Y. Dai, 2007: Impact of vegetation removal and soil aridation on diurnal temperature range in a semiarid region: Application to the Sahel. *Proc. Natl. Acad. Sci. USA,* **104,** 17 937–17 942, doi:10.1073/pnas.0700290104.

——, ——, P. Dirmeyer, H. Chen, Y. Dai, and Y. Tian, 2008: Asymmetric response of maximum and minimum temperatures to soil emissivity change over the Northern African Sahel in a GCM. *Geophys. Res. Lett.,* **35,** L05402, doi:10.1029/2007GL032953.